Selective Activation of One Methyl Ketone Enantioface via σ-Binding to a Chiral Transition-Metal Template: Synthesis, Structure, and Reactivity of Rhenium Ketone Complexes $[(\eta^5\text{-}C_5H_5)Re(NO)(PPh_3)(\eta^1\text{-}O{=}C(CH_3)R)]^+X^-$

Dennis M. Dalton,[1a] Jesús M. Fernández,[1a] Kenneth Emerson,[1b] Raymond D. Larsen,[1b] Atta M. Arif,[1a] and J. A. Gladysz*,[1a]

Contribution from the Departments of Chemistry, University of Utah, Salt Lake City, Utah 84112, and Montana State University, Bozeman, Montana 59717. *Received May 10, 1990*

Abstract: Reactions of dichloromethane complex $[(\eta^5\text{-}C_5H_5)Re(NO)(PPh_3)(ClCH_2Cl)]^+X^-$ (2^+X^-: $X^- = BF_4^-$, PF_6^-) and O=C(CH$_3$)R (R = (**a**) CH$_3$, (**b**) CH$_2$CH$_3$, (**c**) CH(CH$_3$)$_2$, (**d**) C(CH$_3$)$_3$; (**e**) C$_6$H$_5$) give σ ketone complexes $[(\eta^5\text{-}C_5H_5)Re(NO)(PPh_3)(\eta^1\text{-}O{=}C(CH_3)R)]^+X^-$ (**3a-e**$^+X^-$, 79-89%). Crystal structures (**3a,e**$^+PF_6^-$) show N-Re-O-C torsion angles of 21-9°, one C=O face to be shielded by the bulky PPh$_3$ ligand, and rhenium cis to CH$_3$. The *E*/*Z* methyl groups in **3a**$^+BF_4^-$ rapidly exchange ($\Delta G^{\ddagger}_{133K}$ = 6 kcal/mol). Both K(*sec*-C$_4$H$_9$)$_3$BH and formyl complex $(\eta^5\text{-}C_5H_5)Re(NO)(PPh_3)(CHO)$ (**7**) reduce **3a-e**$^+X^-$ to alkoxide complexes (*RS*,*SR*)-$(\eta^5\text{-}C_5H_5)Re(NO)(PPh_3)(OCH(CH_3)R)$ (**5**) in high yields and 75-99% de. The structure of (*RS*,*SR*)-**5e** is verified crystallographically and is consistent with hydride addition from a direction anti to the PPh$_3$ ligand. Analogous reactions starting with optically active **2**$^+BF_4^-$ give optically active ketone and alkoxide complexes with retention of configuration at rhenium. Reactions of (+)-(*RS*)-**5b-e**, (+)-(*S*)-C$_6$H$_5$(CH$_3$O)(F$_3$C)CC(=O)Cl, and 4-(dimethylamino)pyridine give esters (*RS*)-C$_6$H$_5$(CH$_3$O)(F$_3$C)CC(=O)OCH(CH$_3$)R (95-99%) in de that closely match those of (+)-(*RS*)-**5b-e**. Reactions of (+)-(*RS*)-**5c,d** and (-)-(*S*)-C$_6$H$_5$(CH$_3$O)(F$_3$C)CC(=O)OH give alcohols (*S*)-HOCH(R)CH$_3$ and carboxylate complex (+)-(*RS*)-$(\eta^5\text{-}C_5H_5)Re(NO)(PPh_3)(OC(=O)C(CF_3)(OCH_3)C_6H_5)$ (92-93%, ≥99% de). Reaction of (+)-(*RS*)-**5e** with HBF$_4$·O(C$_2$H$_5$)$_2$ and then 2-butanone gives 1-phenylethanol (71%) and (+)-(*RS*)-**3b**$^+BF_4^-$ (78%, 93% ee).

Unsaturated organic molecules are often activated toward nucleophilic addition upon coordination to a transition metal.[2] Surprisingly, however, there have been few if any systematic studies of reactions of ketone complexes and nucleophiles—or for that matter the binding of ketone ligands to inorganic and organometallic fragments.[3] This is remarkable in view of the considerable effort that has been directed at the asymmetric reduction of unsymmetrical ketones to optically active secondary and tertiary alcohols.[4-6] Many classes of chiral metal complexes are now readily available in optically active form[7] and would seem to offer excellent prospects for a general solution to this important problem in organic synthesis.

Scheme I. Synthesis of Ketone Complexes $[(\eta^5\text{-}C_5H_5)Re(NO)(PPh_3)(\eta^1\text{-}O{=}C(CH_3)R)]^+BF_4^-$ ($3^+BF_4^-$)

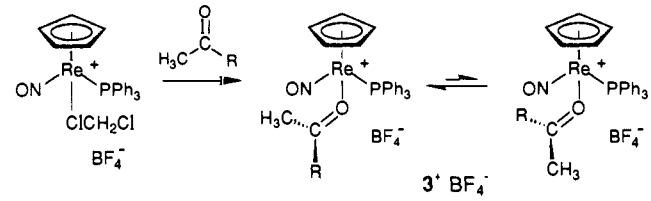

We have shown that "chiral-at-rhenium" complexes of the general formula $[(\eta^5\text{-}C_5H_5)Re(NO)(PPh_3)(L)]^{n+}$ are easily prepared in optically pure form[8] and undergo a variety of reactions in which new ligand-based stereogenic centers are formed with high stereoselectivity.[9-11] In particular, the corresponding cationic aldehyde complexes have been found to undergo highly stereoselective nucleophile additions to give complexes of chiral alkoxides.[10] Thus, we sought to synthesize and study the reactivity of analogous ketone complexes.

(1) (a) University of Utah. (b) Montana State University.

(2) Collman, J. P.; Hegedus, L. S.; Norton, J. R.; Finke, R. G. *Principles and Applications of Organotransition Metal Chemistry*; University Science Books: Mill Valley, CA; Chapter 7.

(3) Huang, Y.-H.; Gladysz, J. A. *J. Chem. Educ.* **1988**, *65*, 298.

(4) Reviews: (a) Midland, M. M. *Chem. Rev.* **1989**, *89*, 1553. (b) Grandbois, E. R.; Howard, S. I.; Morrison, J. D. In *Asymmetric Synthesis*; Morrison, J. D., Ed.; Academic Press: New York, 1983; Vol. 2, pp 71-90. (c) Koenig, K. E. *Ibid.* Vol. 5; pp 79-80.

(5) This literature is extensive. Selected lead references to methods that employ stoichiometric quantities of the chiral reagent or auxiliary: (a) Noyori, R.; Tomino, I.; Tanimoto, Y.; Nishizawa, M. *J. Am. Chem. Soc.* **1984**, *106*, 6709, 6717. (b) Midland, M. M.; Kazubski, A. *J. Org. Chem.* **1982**, *47*, 2495. (c) Itsuno, S.; Nakano, M.; Miyazaki, K.; Masuda, H.; Ito, K.; Hirao, A.; Nakahama, S. *J. Chem. Soc., Perkin Trans. 1* **1985**, 2039. (d) Imai, T.; Tamura, T.; Yamamuro, A.; Sato, T.; Wollmann, T. A.; Kennedy, R. M.; Masamune, S. *J. Am. Chem. Soc.* **1986**, *108*, 7402. (e) Brown, H. C.; Park, W. S.; Cho, B. T.; Ramachandran, P. V. *J. Org. Chem.* **1987**, *52*, 5406. (f) Brown, H. C.; Chandrasekharan, J.; Ramachandran, P. V. *J. Am. Chem. Soc.* **1988**, *110*, 1539. (g) Brown, H. C.; Ramachandran, P. V. *J. Org. Chem.* **1989**, *54*, 4504.

(6) Lead references to methods that employ catalytic quantities of the chiral reagent or auxiliary: (a) Keinan, E.; Hafeli, E. K.; Seth, K. K.; Lamed, R. *J. Am. Chem. Soc.* **1986**, *108*, 162. (b) Kitamura, M.; Okhuma, T.; Inoue, S.; Sayo, N.; Kumobayashi, H.; Akutagawa, S.; Ohta, T.; Takaya, H.; Noyori, R. *J. Am. Chem. Soc.* **1988**, *110*, 629. (c) Corey, E. J.; Bakshi, R. K.; Shibata, S. *Ibid.* **1987**, *109*, 5551. (d) Corey, E. J.; Bakshi, R. K.; Shibata, S.; Chen, C.-P.; Singh, V. K. *Ibid.* **1987**, *109*, 7925. (e) Corey, E. J.; Chen, C.-P.; Reichard, G. A. *Tetrahedron Lett.* **1989**, *30*, 5547. (f) Shen, G.-W.; Wang, Y.-F.; Bradshaw, C.; Wong, C.-H. *J. Chem. Soc., Chem. Commun.* **1990**, 677. (g) Takahashi, H.; Sakurada, S.; Takeda, H.; Achiwa, K. *J. Am. Chem. Soc.* **1990**, *112*, 5876.

(7) See articles published in "Organometallic Compounds and Optical Activity". *J. Organomet. Chem.* **1989**, *370*; Brunner, H., volume editor.

(8) Merrifield, J. H.; Strouse, C. E.; Gladysz, J. A. *Organometallics* **1982**, *1*, 1204.

(9) Some lead references: (a) O'Connor, E. J.; Kobayashi, M.; Floss, H. G.; Gladysz, J. A. *J. Am. Chem. Soc.* **1987**, *109*, 4837. (b) Bodner, G. S.; Smith, D. E.; Hatton, W. G.; Heah, P. C.; Georgiou, S.; Rheingold, A. L.; Geib, S. J.; Hutchinson, J. P.; Gladysz, J. A. *Ibid.* **1987**, *109*, 7688. (c) Senn, D. R.; Wong, A.; Patton, A. T.; Marsi, M.; Strouse, C. E.; Gladysz, J. A. *Ibid.* **1988**, *110*, 6096. (d) Crocco, G. L.; Lee, K. E.; Gladysz, J. A. *Organometallics* **1990**, *9*, 2819. (e) Peng, T.-S.; Gladysz, J. A. *Tetrahedron Lett.* **1990**, *31*, 4417.

(10) (a) Fernández, J. M.; Emerson, K.; Larsen, R. D.; Gladysz, J. A. *J. Am. Chem. Soc.* **1986**, *108*, 8268. (b) Garner, C. M.; Fernández, J. M.; Gladysz, J. A. *Tetrahedron Lett.* **1989**, *30*, 3931. (c) Garner, C. M.; Quirós Méndez, N.; Kowalczyk, J. J.; Fernández, J. M.; Emerson, K.; Larsen, R. D.; Gladysz, J. A. *J. Am. Chem. Soc.* **1990**, *112*, 5146.

(11) Dewey, M. A.; Arif, A. M.; Gladysz, J. A. Manuscript in preparation.

0002-7863/90/1512-9198$02.50/0

The optically active methyl complex $(\eta^5\text{-}C_5H_5)Re(NO)(PPh_3)(CH_3)$ (**1**) is easily converted to the optically active dichloromethane complex $[(\eta^5\text{-}C_5H_5)Re(NO)(PPh_3)(ClCH_2Cl)]^+X^-$ ($\mathbf{2}^+X^-$).[12] Complex $\mathbf{2}^+X^-$ reacts with a variety of donor ligands (L) between −50 and −30 °C to give substitution products $[(\eta^5\text{-}C_5H_5)Re(NO)(PPh_3)(L)]^+X^-$ in high yields and with retention of configuration at rhenium. Hence, $\mathbf{2}^+X^-$ serves as the functional equivalent of the chiral Lewis acid $[(\eta^5\text{-}C_5H_5)Re(NO)(PPh_3)]^+$ (**I**). In this paper, we report (1) the conversion of racemic and optically active **1** to racemic and optically active σ methyl ketone complexes $[(\eta^5\text{-}C_5H_5)Re(NO)(PPh_3)(\eta^1\text{-}O{=}C(CH_3)R)]^+X^-$ ($\mathbf{3}^+X^-$) in high chemical and optical yields, (2) crystal structures of the acetone and acetophenone complexes, which show one C=O face to be shielded by the bulky PPh_3 ligand, (3) dynamic properties of the ketone ligands in solution, (4) highly diastereoselective and enantioselective reductions of $\mathbf{3}^+X$ to racemic and optically active alkoxide complexes $(\eta^5\text{-}C_5H_5)Re(NO)(PPh_3)(OCH(CH_3)R)$, (5) reactions of optically active alkoxide complexes that give esters or alcohols and rhenium complexes in high chemical and optical yields, and (6) mechanistic analyses of the preceding reactions. Portions of this study have been communicated.[13]

Results

1. Synthesis of Ketone Complexes. Methyl complex $(\eta^5\text{-}C_5H_5)Re(NO)(PPh_3)(CH_3)$ (**1**)[14] and $HBF_4{\cdot}O(C_2H_5)_2$ were combined in CH_2Cl_2 at −80 °C as previously described to give the dichloromethane complex $[(\eta^5\text{-}C_5H_5)Re(NO)(PPh_3)(ClCH_2Cl)]^+BF_4^-$ ($\mathbf{2}^+BF_4^-$).[12] Then the methyl ketones (a) acetone, (b) 2-butanone, (c) 3-methyl-2-butanone, (d) 3,3-dimethyl-2-butanone, and (e) acetophenone were added (3 equiv; Scheme I). Workup gave σ ketone complexes $[(\eta^5\text{-}C_5H_5)Re(NO)(PPh_3)(\eta^1\text{-}O{=}C(CH_3)R)]^+BF_4$ (**3a–e**$^+BF_4^-$) in 79–86% yields as orange or red powders. The hexafluorophosphate salts **3a,b,e**$^+PF_6^-$ were analogously prepared from **1** and $HPF_6{\cdot}O(C_2H_5)_2$.[15]

When the preceding reactions were monitored by ^{31}P NMR, ketone complexes $\mathbf{3}^+X^-$ were observed to form over the course of several hours at −40 °C. A k_{obs} for the appearance of **3a**$^+BF_4^-$ was measured at −36 °C in a reaction with 4 equiv of acetone (2.7×10^{-4} s^{-1}). This gave a half-life of 43 min.

Complexes **3a–e**$^+X^-$ were characterized by microanalyses (Experimental Section) and by IR and NMR (^1H, $^{13}C\{^1H\}$, $^{31}P\{^1H\}$) spectroscopy (Table I). The σ ketone coordination mode was assigned from the medium-strong IR $\nu_{C=O}$ at 1554–1625 cm^{-1} and characteristic carbonyl ^{13}C NMR resonances at 216–240 ppm (Table I).[3] Interestingly, reactions of $\mathbf{2}^+BF_4^-$ and *aliphatic* aldehydes[10] gave exclusively π aldehyde complexes $[(\eta^5\text{-}C_5H_5)Re(NO)(PPh_3)(\eta^2\text{-}O{=}CHR)]^+BF_4^-$ ($\mathbf{4}^+BF_4^-$).[16] The IR ν_{NO} of ketone complexes **3a–e**$^+BF_4^-$ (1677–1697 cm^{-1}) were *lower* than those of aldehyde complexes $\mathbf{4}^+BF_4^-$ (1729–1740 cm^{-1}). Also, the PPh_3 ^{31}P NMR resonances of **3a–e**$^+BF_4^-$ were *downfield* of those of $\mathbf{4}^+BF_4^-$ (18.4–18.9 vs 10.0–10.2 ppm). The cyclopentadienyl ^1H and ^{13}C NMR resonances were upfield of those of $\mathbf{4}^+BF_4^-$ (δ 5.59–5.71 vs 5.83–5.96 and 92.9–93.3 vs 98.3–99.3 ppm).

Solutions of the aliphatic ketone complexes **3a–d**$^+BF_4^-$ were orange, while those of acetophenone complex **3e**$^+BF_4^-$ were red. The UV/visible spectra showed intense UV absorptions that tailed into the visible. The spectrum of acetone complex **3a**$^+BF_4^-$ (CH_2Cl_2) exhibited small shoulders at 312 and 364 nm (ε 2200, 1600 M^{-1} cm^{-1}). That of acetophenone complex **3e**$^+BF_4^-$ showed a distinctive visible absorption at 433 nm (ε 5300) and a UV shoulder at 260 nm (ε 18 700).

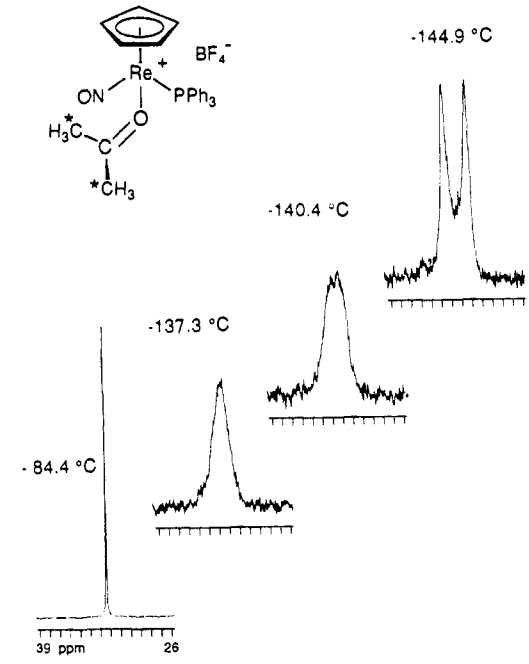

Figure 1. Variable-temperature ^{13}C NMR spectra of labeled acetone complex $[(\eta^5\text{-}C_5H_5)Re(NO)(PPh_3)(\eta^1\text{-}O{=}C(^{13}CH_3)_2)]^+BF_4^-$ (**3a**$^+$-$^{13}C_2BF_4^-$) in $CDFCl_2$.

2. Ketone Ligand Exchange and Isomerism. Unsymmetrical ketone complexes **3b–e**$^+X^-$ can exist as either *E* or *Z* C=O geometric isomers. In the former, the rhenium is cis to the smaller methyl substituent. Thus, it was anticipated that *E* geometric isomers would predominate. Accordingly, **3b–e**$^+X^-$ *appeared* homogenous. No "doubling" or structure associated with the IR ν_{NO} or $\nu_{C=O}$ was noted. Also, no decoalesence phenomena were noted in ^1H NMR spectra recorded at −95 °C.

However, acetone complex **3a**$^+BF_4^-$ exhibited only *one* methyl ^1H and ^{13}C NMR resonance, when in theory separate signals should be observed for the groups cis and trans to the rhenium. Hence, some process must equivalence the *E*/*Z* methyl groups. One possibility would be acetone ligand dissociation. Thus, the rate of reaction of **3a**$^+BF_4^-$ and acetone-d_6 (16 equiv, CD_2Cl_2, 28 °C) was measured. Deuterioacetone complex **3a**$^+$-d_6-BF_4^- formed with $k_{obs} = 1.05 \pm 0.05 \times 10^{-4}$ s^{-1}, corresponding to a half-life of 1.8 h.[17] This shows that the acetone ligand in **3a**$^+BF_4^-$ does not undergo particularly rapid exchange at room temperature.

Efforts to decoalesce the methyl ^1H and ^{13}C NMR resonances of **3a**$^+BF_4^-$ were unsuccessful. Thus, the bis-^{13}C-labeled acetone complex $[(\eta^5\text{-}C_5H_5)Re(NO)(PPh_3)(\eta^1\text{-}O{=}C(^{13}CH_3)_2)]^+BF_4^-$ (**3a**$^+$-$^{13}C_2BF_4^-$) was prepared from $\mathbf{2}^+BF_4^-$ and acetone-*1,3*-$^{13}C_2$. Next, ^{13}C NMR spectra of **3a**$^+$-$^{13}C_2BF_4^-$ were recorded in $CDFCl_2$, as shown in Figure 1. This solvent (mp −135 °C) has been found to easily supercool to −150 °C.[18] The methyl resonances decoalesced at −140 °C, indicating a $\Delta G^{\ddagger}_{133K}$ of only 6.0 ± 0.1 kcal/mol.[19] Hence, *E*/*Z* C=O geometric isomers of unsymmetrical ketone complexes **3b–e**$^+X^-$ should interconvert with similarly low barriers and would not be distinguishable under conventional NMR conditions.

We also sought to assay for π isomers of $\mathbf{3}^+X^-$. Careful inspection of the IR ν_{NO} region (see above; CH_2Cl_2 or CH_3NO_2)[16]

(12) Fernández, J. M.; Gladysz, J. A. *Organometallics* **1989**, *8*, 207.
(13) (a) Fernández, J. M.; Emerson, K.; Larsen, R. L.; Gladysz, J. A. *J. Chem. Soc., Chem. Commun.* **1988**, 37. (b) Dalton, D. M.; Gladysz, J. A. *J Organomet. Chem.* **1989**, *370*, C17.
(14) Tam, W.; Lin, G.-Y.; Wong, W.-K.; Kiel, W. A.; Wong, V. K.; Gladysz, J. A. *J. Chem. Soc.* **1982**, *104*, 141.
(15) At an early stage of this study, the quality of $HPF_6{\cdot}O(C_2H_5)_2$ available from commercial sources declined dramatically, and $\mathbf{2}^+PF_6^-$ could only be generated in low spectroscopic yields. Accordingly, we standardized on tetrafluoroborate salts $\mathbf{3}^+BF_4^-$ for reactivity studies.
(16) (a) In aromatic aldehyde complexes $[(\eta^5\text{-}C_5H_5)Re(NO)(PPh_3)(O{=}CHAr)]^+BF_4^-$, either the π or σ binding mode can dominate. This is a sensitive function of arene substituents, temperature, and solvent.[16b] (b) Quirós Méndez, N.; Arif, A. M.; Gladysz, J. A. *Angew. Chem., Int. Ed. Engl.*, in press.
(17) The first-order k_{obs} is consistent with either a dissociative or associative exchange mechanism: Espenson, J. H. *Chemical Kinetics and Reaction Mechanisms*; McGraw Hill: New York, 1981; pp 50–55. Experiments to distinguish these possibilities are planned.
(18) Siegel, J. S.; Anet, F. A. L. *J. Org. Chem.* **1988**, *53*, 2629.
(19) Sandström, J. *Dynamic NMR Spectroscopy*; Academic Press: New York, 1982; Chapter 7.

Chart I[a]

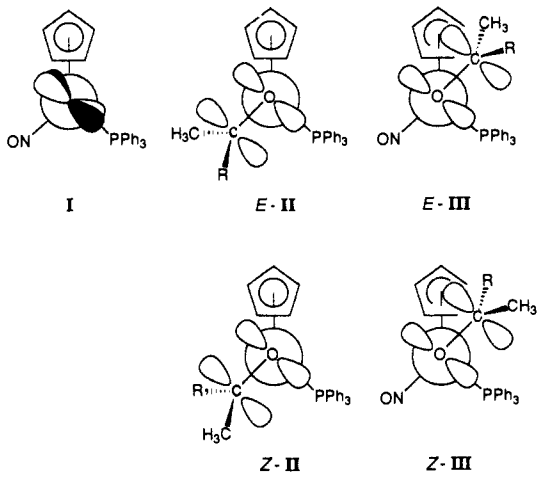

[a] I: Pyramidal rhenium fragment $[(\eta^5\text{-}C_5H_5)Re(NO)(PPh_3)]^+$ with d orbital HOMO. II and III: Newman-type projections of possible Re–O conformations of σ ketone complexes $\mathbf{3}^+X^-$. *E* and *Z* designate geometric isomers about the C=O bond.

showed no absorptions or shoulders that could be attributed to π isomers, within the limits of detection (≤4%). Also, π isomers would exhibit characteristic C–O ^{13}C NMR chemical shifts (70–100 ppm)[3,10,16] and increase in concentration upon cooling.[16] Thus, the *carbonyl*-labeled acetone complex $[(\eta^5\text{-}C_5H_5)Re(NO)(PPh_3)(\eta^1\text{-}O{=}{}^{13}C(CH_3)_2)]^+BF_4^-$ ($\mathbf{3a}^{+}\text{-}{}^{13}C BF_4^-$) was prepared, and ^{13}C NMR spectra were recorded as in Figure 1. The carbonyl resonance shifted only slightly between 20 (238.0 ppm) and −130 °C (235.6 ppm). No decoalesence of a π acetone resonance was observed, within the limits of detection (≤1%; signal/noise 313). As expected, the IR ν_{CO} of $\mathbf{3a}^{+}\text{-}{}^{13}CBF_4^-$ (KBr, 1582 cm^{-1}, m) was lower than that of $\mathbf{3a}^+BF_4^-$ (1618 cm^{-1}).

3. Solid-State Structures of Ketone Complexes. The Lewis acid fragment $[(\eta^5\text{-}C_5H_5)Re(NO)(PPh_3)]^+$ has been shown to be a strong π base, with the high-lying d orbital HOMO shown in I (Chart I).[20] Unsaturated ligands generally adopt conformations that allow considerable overlap of their acceptor orbitals with this donor orbital.[9c,10,20-22] Although σ ketone ligands are not strong π acceptors,[23] they might nonetheless be expected to adopt conformations of the types II and III, shown in Chart I. These idealized structures exhibit N–Re–O–C torsion angles of 0° and 180°, respectively, and maximize overlap of the C=O π^* orbital lobes on oxygen with the d orbital shown in I. In the former, one ketone substituent is projected at the small nitrosyl ligand, but a slight torsional distortion should relieve any interaction. In the latter, a ketone substituent is projected into the region between the large PPh_3 ligand and the medium-sized cyclopentadienyl ligand. With either rotamer, *E* C=O geometric isomers should be more stable.

X-ray data were acquired on acetone complex $\mathbf{3a}^+PF_6^-$ and acetophenone complex $\mathbf{3e}^+PF_6^-$ as summarized in Table II. Refinement, described in the Experimental Section, yielded the structures shown in Figures 2 and 3. As expected, $\mathbf{3e}^+PF_6^-$ crystallized as an *E* C=O geometric isomer. Bond lengths and angles are summarized in Table III, and atomic coordinates and anisotropic thermal parameters are given in the supplementary material.

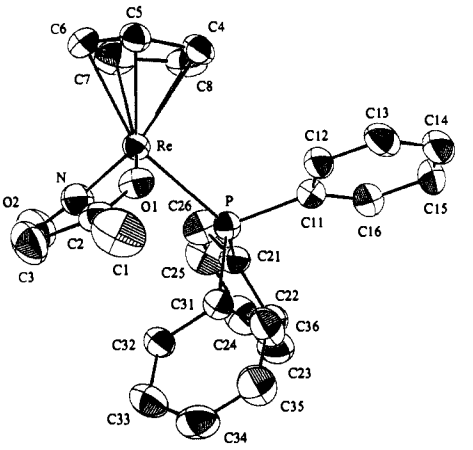

Figure 2. Structure of the cation of acetone complex $[(\eta^5\text{-}C_5H_5)Re(NO)(PPh_3)(\eta^1\text{-}O{=}C(CH_3)_2)]^+PF_6^-$ ($\mathbf{3a}^+PF_6^-$).

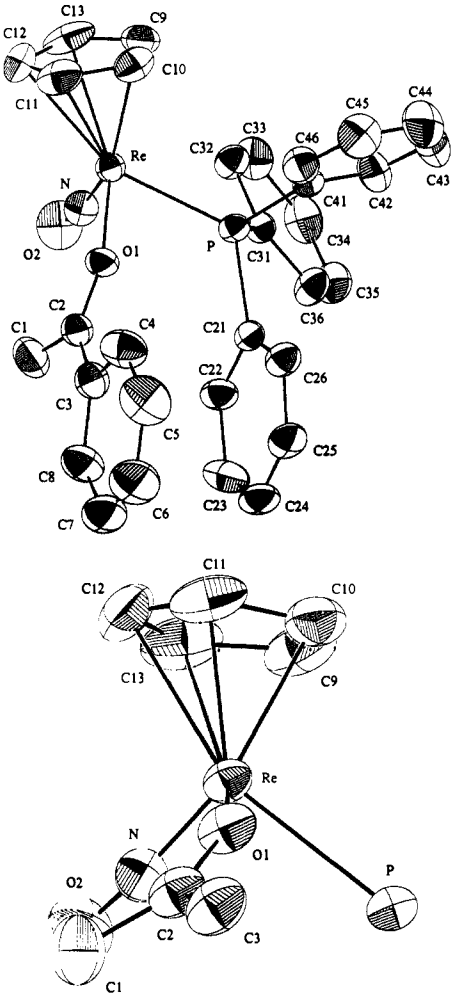

Figure 3. Views of the cation of acetophenone complex $[(\eta^5\text{-}C_5H_5)Re(NO)(PPh_3)(\eta^1\text{-}O{=}C(CH_3)C_6H_5)]^+PF_6^-$ ($\mathbf{3e}^+PF_6^-$). Top: Numbering diagram. Bottom: View down the oxygen–rhenium bond with phenyl rings omitted.

Complexes $\mathbf{3a,e}^+PF_6^-$ exhibited N–Re–O–C torsion angles of 21° and 9°, respectively—closely matching that of idealized conformer II. Also, the acetophenone phenyl ring in $\mathbf{3e}^+PF_6^-$ and a PPh_3 ligand phenyl ring were conspicuously parallel (Figure 3). The respective least-squares planes made a 4° angle, and atom/plane distances ranged from 3.06 to 3.27 Å. The acetophenone phenyl ring was also nearly parallel to the plane defined by the carbonyl fragment C1/C2/O1 (∠12°), evidencing a high degree of conjugation. Accordingly, ν_{CO} for $\mathbf{3e}^+X^-$ (1554–1558 cm^{-1}) is much lower than aliphatic ketone complexes $\mathbf{3a–d}^+X^-$ (1605–1625 cm^{-1}).

(20) (a) Kiel, W. A.; Lin, G.-Y.; Constable, A. G.; McCormick, F. B.; Strouse, C. E.; Eisenstein, O.; Gladysz, J. A. *J. Am. Chem. Soc.* **1982**, *104*, 4865. (b) Georgiou, S.; Gladysz, J. A. *Tetrahedron* **1986**, *42*, 1109.

(21) Bodner, G. S.; Patton, A. T.; Smith, D. E.; Georgiou, S.; Tam, W.; Wong, W.-K.; Strouse, C. E.; Gladysz, J. A. *Organometallics* **1987**, *6*, 1954.

(22) (a) Bodner, G. S.; Fernández, J. M.; Arif, A. M.; Gladysz, J. A. *J. Am. Chem. Soc.* **1988**, *110*, 4082. (b) Bodner, G. S.; Peng, T.-S.; Arif, A. M.; Gladysz, J. A. *Organometallics* **1990**, *9*, 1191.

(23) Calculated energies of frontier orbitals in acetaldehyde and acetone (eV): π, −13.46, −13.00; n, −11.31, −10.93; π^*, 4.39, 4.53. Wu, Y.-O.; Houk, K. N. Unpublished results, UCLA. See also: Vedejs, E.; Perry, D. A.; Houk, K. N.; Rondan, N. G. *J. Am. Chem. Soc.* **1983**, *105*, 6999.

Table I. Spectroscopic Characterization of Ketone Complexes $[(\eta^5\text{-}C_5H_5)Re(NO)(PPh_3)(\eta^1\text{-}O{=}C(CH_3)R)]^+BF_4^-$ ($\mathbf{3}^+BF_4^-$) and Alkoxide Complexes (*RS,SR*)-$(\eta^5\text{-}C_5H_5)Re(NO)(PPh_3)(OCH(CH_3)R)$ ((*RS,SR*)-**5**)[a]

complex (R)	IR (cm^{-1}, KBr/CH_2Cl_2)	^1H NMR[b,c] (δ)	$^{13}C\{^1H\}$ NMR[c,d] (ppm)	$^{31}P\{^1H\}$ NMR[c,e] (ppm)
3a$^+BF_4^-$ (CH_3)	ν_{NO} 1680 vs/1693 vs $\nu_{C=O}$ 1618 m/1622 m	7.59–7.30 (m, $3C_6H_5$), 5.61 (s, C_5H_5), 2.34 (d, J_{HP} = 0.7, $2CH_3$)	PPh_3 at 133.7 (d, J = 10.8), 132.0 (s, *p*), 131.6 (d, J = 40.5, *i*), 129.1 (d, J = 10.8); 231.9 (s, CO), 92.9 (s, C_5H_5), 32.3 (s, $2CH_3$)	18.7 (s)
3b$^+BF_4^-$ (CH_2CH_3)	ν_{NO} 1686 vs/1694 vs $\nu_{C=O}$ 1617 s/1625 m	7.61–7.28 (m, $3C_6H_5$), 5.61 (s, C_5H_5), 2.94 (dq, J = 19.3, 7.1, CHH'), 2.51 (dq, J = 19.3, 7.1, CHH'), 2.38 (s, $COCH_3$), 0.75 (t, J = 7.1, CH_2CH_3)	PPh_3 at 133.8 (d, J = 11.0), 132.0 (d, J = 1.5, *p*), 131.8 (d, J = 55.2, *i*), 129.6 (d, 10.7); 234.9 (s, CO), 92.9 (s, C_5H_5), 39.5 (s, CH_2), 31.1 (s, $COCH_3$), 8.2 (s, CH_2CH_3)	18.9 (s)
3c$^+BF_4^-$ ($CH(CH_3)_2$)	ν_{NO} 1692 vs/1694 vs $\nu_{C=O}$ 1611 s/1614 m	7.60–7.25 (m, $3C_6H_5$), 5.59 (s, C_5H_5), 2.93 (m, CH), 2.45 (s, $COCH_3$), 0.86 (d, J = 6.5, $CHCH_3$), 0.69 (d, J = 7.0, $CHC'H_3$)	PPh_3 at 133.7 (d, J = 11.1), 132.0 (d, J = 55.4, *i*), 131.9 (d, J = 2.5, *p*), 129.5 (d, J = 10.7); 238.2 (d, J = 2.0, CO), 93.0 (d, J = 1.6, C_5H_5), 44.5 (s, $COCH_3$), 29.7 (s, $CH_3CHC'H_3$), 18.9 (s, $CHCH_3$), 17.7 (s, $CHC'H_3$)	18.5 (s)
3d$^+BF_4^-$ ($C(CH_3)_3$)	ν_{NO} 1684 vs/1697 vs $\nu_{C=O}$ 1607 s/1605 m	7.60–7.25 (m, $3C_6H_5$), 5.59 (s, C_5H_5), 2.47 (s, $COCH_3$), 0.87 (s, $C(CH_3)_3$)	PPh_3 at 133.9 (d, J = 11.1), 132.3 (d, J = 55.7, *i*), 132.2 (d, J = 2.4, *p*), 129.8 (d, J = 10.9); 240.4 (s, CO), 93.2 (d, J = 1.5, C_5H_5), 48.1 (s, $C(CH_3)_3$), 27.4 (s, $COCH_3$), 26.6 (s, $C(CH_3)_3$)	18.7 (s)
3e$^+BF_4^-$ (C_6H_5)	ν_{NO} 1677 vs/1693 vs $\nu_{C=O}$ 1558 m/1554 m	7.65–7.25 (m, $4C_6H_5$), 5.71 (s, C_5H_5), 2.62 (d, J_{HP} = 0.5, CH_3)	PPh_3 at 133.8 (d, J = 10.8), 132.0 (d, J = 1.7, *p*), 131.3 (d, J = 55.7, *i*), 129.6 (d, J = 10.8); CPh at 136.4 (s), 135.0 (s), 129.7 (s), 129.3 (s); 215.9 (s, CO), 93.3 (s, C_5H_5), 26.8 (s, CH_3)	18.4 (s)
5a (CH_3)	ν_{NO} 1613 vs	7.77–6.99 (m, $3C_6H_5$), 4.85 (s, C_5H_5), 3.65 (sp, J = 5.9, OCH), 1.36 (d, J = 5.9, CH_3), 1.11 (d, J = 5.9, $'CH_3$)	PPh_3 at 135.7 (d, J = 50.6, *i*), 134.6 (d, J = 10.3), 130.2 (d, J = 2.1, *p*), 128.2 (d);[f] 90.7 (d, J = 2.1, C_5H_5), 84.7 (d, J = 6.4, OC), 27.3 (s, CH_3), 27.0 (s, $'CH_3$)	16.6 (s)
(*RS,SR*)-**5b** (CH_2CH_3)	ν_{NO} 1612 vs	7.77–7.02 (m, $3C_6H_5$), 4.86 (s, C_5H_5), 3.37 (m, OCH), 1.39 (d, J = 6.0, $COCH_3$), 1.39 (m, CH_2), 0.91 (t, J = 7.2, CH_2CH_3)	PPh_3 at 136.2 (d, J = 50.5, *i*), 134.6 (d, J = 10.4), 130.2 (d, J = 2.0, *p*), 128.3 (d);[f] 90.8 (d, J = 2.1, C_5H_5), 89.8 (d, J = 6.2, OC), 34.4 (s, CH_2), 25.0 (s, $COCH_3$), 11.6 (s, CH_2CH_3)	16.9 (s)
(*RS,SR*)-**5c** ($CH(CH_3)_2$)	ν_{NO} 1627 vs	7.80–6.90 (m, $3C_6H_5$), 4.86 (s, C_5H_5), 3.23 (m, OCH), 1.52 (m, $CH(CH_3)_2$), 1.38 (d, J = 6.2, $COCH_3$), 0.89 (d, J = 6.7, $CHCH_3$), 0.80 (d, J = 6.8, $CHC'H_3$)	PPh_3 at 135.7 (d, J = 49.6, *i*), 134.6 (d, J = 10.4), 130.2 (s, *p*), 128.2 (d);[f] 93.2 (d, J = 5.9, OC), 90.7 (s, C_5H_5), 37.1 (s), 21.8 (s), 20.2 (s), 18.0 (s)	17.6 (s)
(*RS,SR*)-**5d** ($C(CH_3)_3$)	ν_{NO} 1604 vs	7.70–6.90 (m, $3C_6H_5$), 4.88 (s, C_5H_5), 3.10 (q, J = 6.0, OCH), 1.40 (d, J = 6.0, $COCH_3$), 0.85 (s, $C(CH_3)_3$)	PPh_3 at 135.6 (d, J = 50.4, *i*), 134.6 (d, J = 10.6), 130.2 (s, *p*), 128.5 (d);[f] 96.4 (d, J = 5.8, OC), 90.7 (s, C_5H_5), 37.2 (s, $C(CH_3)_3$), 26.9 (s, $C(CH_3)_3$), 19.1 (s, $COCH_3$)	18.6 (s)
(*RS,SR*)-**5e** (C_6H_5)	ν_{NO} 1632 vs	7.76–7.02 (m, $4C_6H_5$), 4.79 (s, C_5H_5), 4.65 (q, J = 6.0, OCH), 1.59 (d, J = 6.2, CH_3)	PPh_3 at 135.6 (d, J = 50.7, *i*), 134.6 (d, J = 10.5), 130.3 (d, J = 2.2, *p*), 128.6 (d);[f] CPh at 126.1 (s), 125.9 (s);[g] 92.7 (d, J = 6.0, CH), 90.5 (d, J = 2.0, C_5H_5), 28.3 (s, CH_3)	18.3 (s)

[a] Partial data on diastereomers (*RR,SS*)-**5b–e** are given in the experimental section. [b] At 300 MHz and ambient probe temperature and referenced to internal $(CH_3)_4Si$; all couplings (Hz) are to hydrogen unless noted. [c] NMR solvents: **3a–e**$^+BF_4^-$, CD_2Cl_2; (*RS,SR*)-**5a–e**, C_6D_6. [d] At 75 MHz and ambient probe temperature and referenced to internal $(CH_3)_4Si$; all couplings (Hz) are to phosphorus unless noted. [e] At 121 MHz and ambient probe temperature and referenced to external 85% H_3PO_4. [f] One line of doublet obscured by solvent. [g] Two phenyl carbons obscured by solvent.

4. Reduction of Ketone Complexes to Alkoxide Complexes. Hydride additions to π aldehyde complexes $[(\eta^5\text{-}C_5H_5)Re(NO)(PPh_3)(\eta^2\text{-}O{=}CHR)]^+X^-$ ($\mathbf{4}^+X^-$) have been extensively studied.[10] The resulting *primary* alkoxide complexes $(\eta^5\text{-}C_5H_5)Re(NO)(PPh_3)(OCH_2R)$ are very sensitive toward rhenium–oxygen bond cleavage by electrophiles, including byproducts commonly generated by hydride donors.[10] Analogous deuteride additions give α-deuterioalkoxide complexes $(\eta^5\text{-}C_5H_5)Re(NO)(PPh_3)(OCHDR)$ in high diastereomeric excesses.

We sought to similarly reduce σ ketone complexes $\mathbf{3}^+X^-$ to *secondary* alkoxide complexes $(\eta^5\text{-}C_5H_5)Re(NO)(PPh_3)(OCH(R)CH_3)$ (**5**). This would generate a new asymmetric carbon and could potentially occur with high 1,3-asymmetric induction. We also sought reaction conditions that would leave the rhenium–oxygen bond of **5** intact. This would enable reduction stereoselectivities to be determined by NMR analysis of the alkoxide complex diastereomer ratios.

Dichloromethane solutions of $\mathbf{3}^+BF_4^-$ were treated with $Li(C_2H_5)_3BH$ at −80 °C. A multitude of products formed, as assayed by ^{31}P NMR. A major resonance corresponded to that of $(\eta^5\text{-}C_5H_5)Re(NO)(PPh_3)(Cl)$ (**6**).[24] Similar reductions with $BH_3\cdot THF$ and $NaBH_4$ gave mainly hydride complex $(\eta^5\text{-}C_5H_5)Re(NO)(PPh_3)(H)$.[25] However, reactions of $\mathbf{3}^+BF_4^-$ and

(24) Merrifield, J. H.; Fernández, J. M.; Buhro, W. E.; Gladysz, J. A. *Inorg. Chem.* **1984**, *23*, 4022.

Scheme II. Borohydride Reductions of Racemic and Optically Active Ketone Complexes $3^+BF_4^-$

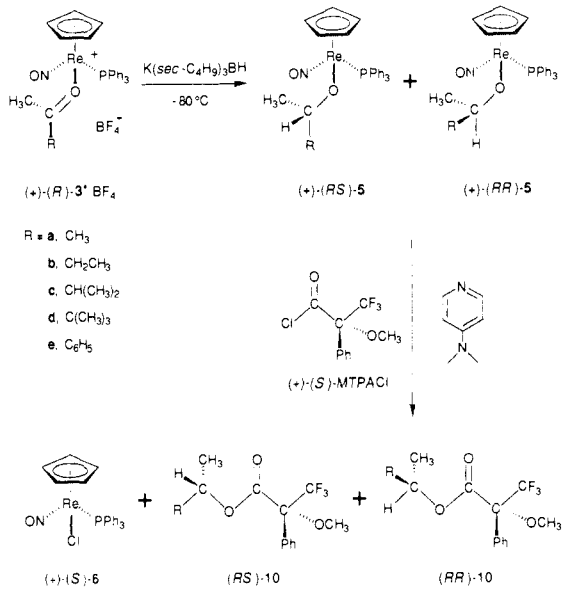

entry	ketone complex	ratio (±)-(RS,SR)-5/(±)-(RR,SS)-5 or (+)-(RS)-5/(+)-(RR)-5		yield (%)	ratio (RS)-10/(RR)-10		yield (%)
1	(±)-(R,S)-3a+ BF_4^-	———		87	———		—
2	(±)-(R,S)-3b+ BF_4^-	87.5:12.5	(75% de)	91	49.0:51.0		80
3	(±)-(R,S)-3c+ BF_4^-	91.0:9.0	(82% de)	92	50.0:50.0		86
4	(±)-(R,S)-3d+ BF_4^-	99.0:1.0	(98% de)	77	49.0:51.0		93
5	(±)-(R,S)-3e+ BF_4^-	98.5:1.5	(97% de)	90	49.0:51.0		98
6	(+)-(R)-3a+ BF_4^-	———		54	———		—
7	(+)-(R)-3b+ BF_4^-	89.0:11.0	(78% de)	89	89.5:10.5	(79% de)	99
8	(+)-(R)-3c+ BF_4^-	95.0:5.0	(90% de)	90	96.5:3.5	(93% de)	97
9	(+)-(R)-3d+ BF_4^-	99.0:1.0	(98% de)	78	99.0:1.0	(98% de)	95
10	(+)-(R)-3e+ BF_4^-	98.5:1.5	(97% de)	92	98.0:2.0	(96% de)	96
11	(-)-(S)-3d+ BF_4^-	99.5:0.5 [a]	(99% de)	73	———		—

[a] (-)-(SR)-5d/(-)-(SS)-5d ratio.

$Li(sec\text{-}C_4H_9)_3BH$ gave appreciable amounts of alkoxide complexes **5** (ca. 66%). This reductant gives the borane byproduct $(sec\text{-}C_4H_9)_3B$, which is bulkier and less Lewis acidic than those produced in the preceding reactions. We speculated that yields might improve further by replacing the lithium ion with the less Lewis acidic potassium ion.

Accordingly, dichloromethane solutions of **3a–e**$^+BF_4^-$ were treated with $K(sec\text{-}C_4H_9)_3BH$ (1.05–1.10 equiv) at −80 °C (Scheme II). Reductions to alkoxide complexes **5a–e** were complete within 3 min at −80 °C, as assayed by ^{31}P NMR. In preparative experiments, extracts were filtered through CaO. This less adsorbing support[26] allowed the elution of **5a–e** but retained the boron-containing byproducts. In contrast, silica and florisil (untreated) cleaved the rhenium–oxygen bonds in **5a–e**. The filtrates gave analytically pure **5a–e** (92–77%) as 99:1 to 87:13 mixtures of (*RS,SR*)/(*RR,SS*) diastereomers.[27,28] Configurations were assigned as described below. Careful analysis of **5c,d** showed that diastereomer ratios were identical before and after workup.

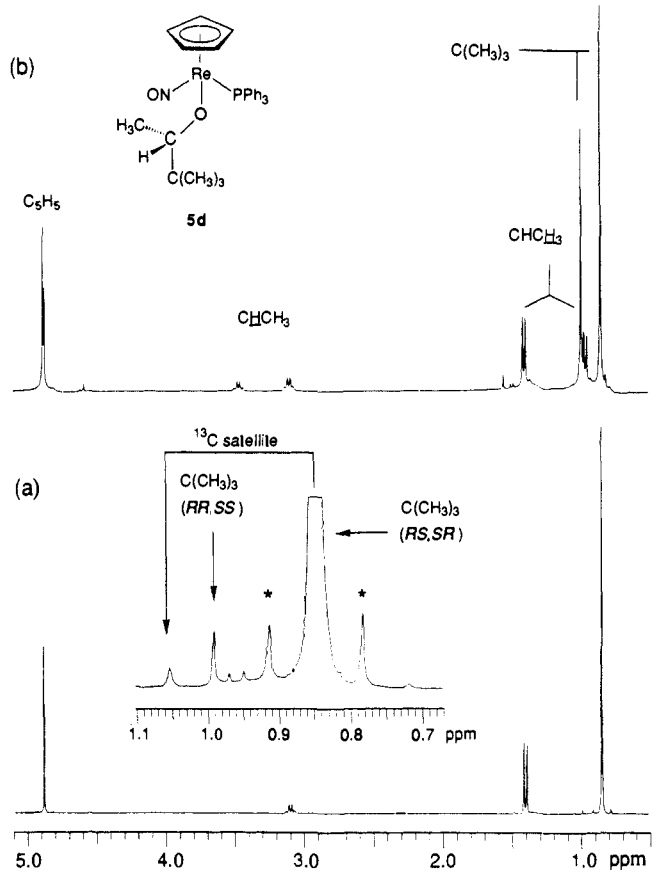

Figure 4. Representative ^1H NMR spectra of diastereomeric alkoxide complexes: (a) A 99:1 (*RS,SR*)/(*RR,SS*)-**5d** mixture from the reaction of **3d**$^+BF_4^-$ and $K(sec\text{-}C_4H_9)_3BH$, side bands in the inset are designated by an asterisk. (b) A 61:39 (*RS/SR*)/(*RR,SS*)-**5d** mixture from the reaction of **2**$^+BF_4^-$ with 3,3-dimethyl-2-butanol and then $(C_2H_5)_3N$.

The preceding samples of **5a–e** were characterized (as mixtures of diastereomers) by microanalyses (Experimental Section) and by IR and NMR spectroscopy (Table I). Only NMR data for the major (*RS,SR*) diastereomers are given in Table I. Resonances of the minor (*RR,SS*) diastereomers were assigned with the aid of independent syntheses described below and are provided in the Experimental Section. The spectroscopic properties of **5a–e** are similar to those reported earlier for the corresponding primary alkoxide complexes.[10a,c]

Figure 4 shows the ^1H NMR spectrum of the 1-(*tert*-butyl)-ethoxide complex **5d** obtained in entry 4 of Scheme II. The high stereoselectivity is evidenced by the comparable areas of the *tert*-butyl resonance of the minor (*RR,SS*) diastereomer and the ^{13}C satellite of the *tert*-butyl resonance of the major (*RS,SR*) diastereomer.[28b]

The effect of temperature upon reduction stereoselectivity was briefly examined. Thus, 3-methyl-2-butanone complex **3c**$^+BF_4^-$ and $K(sec\text{-}C_4H_9)_3BH$ were reacted at −23 °C. Alkoxide complex **5c** formed as a 89.0:11.0 mixture of diastereomers,[28] as opposed to 91.0:9.0 in Scheme II. The 3,3-dimethyl-2-butanone complex **3d**$^+BF_4^-$ and $K(sec\text{-}C_4H_9)_3BH$ were reacted at room temperature. Alkoxide complex **5d** formed as a 93.0:7.0 mixture of diastereomers, as opposed to 99.0:1.0 in Scheme II. Substantial amounts of two byproducts also formed.

The formyl complex $(\eta^5\text{-}C_5H_5)Re(NO)(PPh_3)(CHO)$ (**7**) has been shown to efficiently reduce π aldehyde complexes **4**$^+X^-$ to primary alkoxide complexes $(\eta^5\text{-}C_5H_5)Re(NO)(PPh_3)(OCH_2R)$.[10] The byproduct, carbonyl complex $[(\eta^5\text{-}C_5H_5)Re(NO)(PPh_3)(CO)]^+X^-$ (**8**$^+X^-$), is easily separated and is not Lewis acidic. Hence, ketone complexes **3b,e**$^+BF_4^-$ were treated with **7** at −80 °C. Alkoxide complexes **5b,e** formed as 90.0:10.0 and 94.5:5.5 mixtures of (*RS,SR*)/(*RR,SS*) diastereomers, respectively (Scheme III, entries 1 and 2). These ratios are somewhat lower than those reported for analogous reductions of **3b,e**$^+PF_6^-$ in a

(25) Crocco, G. L.; Gladysz, J. A. *J. Am. Chem. Soc.* **1988**, *110*, 6110.
(26) Strain, H. H. *Chromatographic Adsorption Analysis*; Interscience: New York, 1945; pp 49–50.
(27) Absolute configurations are assigned as described in ref 10c.
(28) (a) The **5b–e** diastereomer ratios in Schemes II–IV were determined from peak heights of ^1H NMR cyclopentadienyl (**5b,d,e**, 300 MHz; **5c**, 500 MHz) *and* methyl resonances (**5b**, CH_2CH_3; **5c**, $CHCH_3$; **5d**, $C(CH_3)_3$; **5e**, $OCCH_3$). Long pulse delays (10–20 s, set from independent T_1 measurements to be $\geq 3 \times T_1$) and careful shimming were used to maximize accuracies. The error limit on each component of a diastereomer ratio is judged to be ±2.0—i.e., 92.0:8.0 ≡ (92.0 ± 2.0):(8.0 ± 2.0). Values are expressed to the nearest half-integer to facilitate conversion to % de. (b) The **5d** diastereomer ratio for entry 4, Scheme II (Figure 4), was checked by two additional methods. First, the *tert*-butyl resonances were cut from an expanded spectrum and weighed (δ 0.85/0.99, 99.1:0.9). Second, the δ 1.05 ^{13}C satellite of the δ 0.85 *tert*-butyl resonance (assumed area ratio, 0.55:100) was similarly weighed relative to the δ 0.99 *tert*-butyl resonance (0.61:1.0). This gave a 99.1:0.9 diastereomer ratio.

Table II. Summary of Crystallographic Data for Acetone Complex $[(\eta^5\text{-}C_5H_5)Re(NO)(PPh_3)(\eta^1\text{-}O{=}C(CH_3)_2)]^+PF_6^-$ (**3a**$^+PF_6^-$), Acetophenone Complex $[(\eta^5\text{-}C_5H_5)Re(NO)(PPh_3)(\eta^1\text{-}O{=}C(CH_3)C_6H_5)]^+PF_6^-$ (**3e**$^+PF_6^-$), and Alkoxide Complex $(RS,SR)\text{-}(\eta^5\text{-}C_5H_5)Re(NO)(PPh_3)(OCH(CH_3)C_6H_5)$ ((*RS,SR*)-**5e**)

	3a$^+PF_6^-$	**3e**$^+PF_6^-$	(*RS,SR*)-**5e**
mol formula	$C_{26}H_{26}F_6NO_2P_2Re$	$C_{31}H_{28}NO_2P_2F_6Re$	$C_{31}H_{29}NO_2PRe$
mol wt	746.7	808.9	664.8
cryst system	monoclinic	monoclinic	monoclinic
space group	$P2_1/n$	$P2_1/n$	$P2_1/c$ (No. 14)
temp of collection, °C	25	25	16
cell dimensions			
a, Å	7.773 (1)	14.348 (2)	9.315 (1)
b, Å	17.688 (3)	15.206 (2)	16.264 (4)
c, Å	20.124 (4)	14.770 (2)	17.922 (2)
β, deg	100.22 (1)	108.44 (1)	100.10 (1)
V, Å^3	2723 (1)	3057.0 (6)	2673.2
Z	4	4	4
d_{calcd}, g/cm^3	1.82	1.76	1.65
cryst dimns, mm	0.12 × 0.25 × 0.36	0.20 × 0.32 × 0.44	0.24 × 0.24 × 0.15
radiation, Å	λ (Mo Kα) 0.71069	λ (Mo Kα) 0.71069	λ (Mo Kα) 0.71069
data collection method	Wyckoff ω	96 step ω	θ–2θ (3°–46°)
scan speed, deg/min	variable, 15–60	variable, 15–60	variable, 3–8
reflcns measured	$\pm h,+k,+l$	$\pm h,+k,+l$	$+h,+k,\pm l$
scan range, deg	2	1	1
total bkgd time/scan time	1	0.20[a]	0.5
no. of reflcns between std	97	97	98
total unique data	7933	10615	4403
obsd data, $I > 3\sigma(I)$	4919	5273	3156
abs coeff (μ), cm^{-1}	49.1	43.9	46.9
min transmission factor	0.48[b]	0.23[c]	0.83[b]
max transmission factor	0.97[b]	0.43[c]	0.99[b]
no. of variables	345	389	325
$R = \sum(\|\|F_o\| - \|F_c\|\|)/\sum\|F_o\|$	0.0402	0.0416	0.0384
$R_w = [\sum w(\|F_o\| - \|F_c\|)^2/\sum w\|F_o\|^2]^{1/2}$	0.0385	0.0408	0.0422
goodness of fit	1.24	1.09	2.64
$\Delta\rho$(max), e/Å^3	1.1, <1.5 Å from Re	0.8, 1.6 Å from P2	1.39
weighting factor w	$K/(\sigma^2(F_o) + 0.0002(F_o)^2)$	$K/(\sigma^2(F_o) + 0.00041(F_o)^2)$	$4(F_o)^2/[\sigma(F_o)^2]^2$

[a] Profile fitting applied. [b] Empirical value. [c] Calculated value.

Scheme III. Formyl Reductions of Racemic and Optically Active Ketone Complexes **3**$^+BF_4^-$

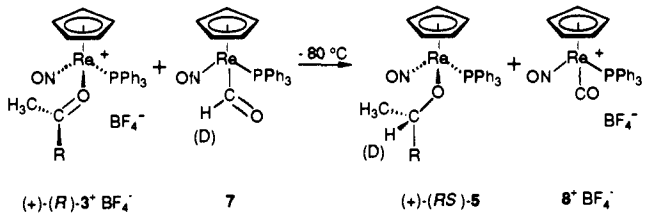

(+)-(*R*)-**3**$^+$ BF_4^- **7** (+)-(*RS*)-**5** **8**$^+$ BF_4^-

R = **b**, CH_2CH_3
e, C_6H_5

entry	ketone complex	formyl complex	ratio (±)-(*RS,SR*)-**5**/(±)-(*RR,SS*)-**5** or (+)-(*RS*)-**5**-d_n/(+)-(*RR*)-**5**-d_n
1	(±)-(*R,S*)-**3b**$^+$ BF_4^-	(±)-**7**	90.0:10.0 (80% de)
2	(±)-(*R,S*)-**3e**$^+$ BF_4^-	(±)-**7**	94.5:5.5 (89% de)
3	(+)-(*R*)-**3b**$^+$ BF_4^-	(±)-**7**	90.5:9.5 (81% de)
4	(+)-(*R*)-**3e**$^+$ BF_4^-	(±)-**7**	98.0:2.0 (96% de)
5	(+)-(*R*)-**3b**$^+$ BF_4^-	(+)-(*S*)-**7**-d_1	97.5:2.5 (95% de)
6	(+)-(*R*)-**3b**$^+$ BF_4^-	(-)-(*R*)-**7**-d_1	83.0:17.0 (66% de)

preliminary communication.[13a,15]

5. Additional Characterization of Alkoxide Complexes. In order to confirm our analysis of the preceding NMR data, we sought authentic samples of alkoxide complexes **5b–e** that contained appreciable amounts of both diastereomers. It has previously been shown that dichloromethane complex **2**$^+BF_4^-$ and primary alcohols RCH_2OH react to give isolable alcohol complexes $[(\eta^5\text{-}C_5H_5)Re(NO)(PPh_3)(HOCH_2R)]^+BF_4^-$.[29] These can in turn be deprotonated to primary alkoxide complexes $(\eta^5\text{-}C_5H_5)Re(NO)(PPh_3)(OCH_2R)$.[29]

Scheme IV. Independent Synthesis of Alkoxide Complexes (*RS,SR*)/(*RR,SS*)-$(\eta^5\text{-}C_5H_5)$Re(NO)(PPh$_3$)(OCH(CH$_3$)R) ((*RS,SR*)/(*RR,SS*)-**5**)

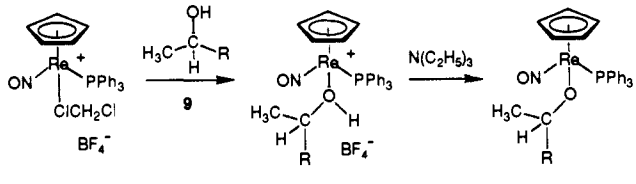

2$^+$ BF_4^- R = **b**, CH_2CH_3; **c**, $CH(CH_3)_2$; **d**, $C(CH_3)_3$; **e**, C_6H_5

	(*RS,SR*)/(*RR,SS*)-**5**
b	53:47
c	77:23
d	61:39
e	82:18

Accordingly, **2**$^+BF_4^-$ was generated in a minimum of dichloromethane and treated with excesses of the secondary alcohols 2-butanol (**9b**), 3-methyl-2-butanol (**9c**), 3,3-dimethyl-2-butanol (**9d**), and 1-phenylethanol (**9e**). The volatiles were removed, and $(C_2H_5)_3N$ was added. Workup gave alkoxide complexes **5b–e** (95–76%) as 53:47, 77:23, 61:39, and 82:18 mixtures of (*RS,SR*)/(*RR,SS*) diastereomers, respectively (Scheme IV).[28a] A ^{1}H NMR spectrum of **5d** prepared by this route is given in Figure 4.

Configurations were assigned to diastereomers of **5b–e** based upon experiments with optically active compounds described below. However, a crystallographic verification was also sought. Thus, 1-phenylethoxide complex (*RS,SR*)-**5e** was crystallized to diastereomeric purity. X-ray data were collected as summarized in Table II. Refinement, described in the Experimental Section, gave the structures shown in Figure 5. Bond lengths and angles are listed in Table III, and atomic coordinates and anisotropic thermal parameters are compiled in the supplementary material. The

(29) Agbossou, S. K.; Smith, W. W.; Gladysz, J. A. *Chem. Ber.* **1990**, *123*, 1293.

Table III. Selected Crystallographic Bond Lengths (Å) and Angles (deg)

A. $3a^+PF_6^-$

Re-O1	2.099 (5)	Re-C4	2.278 (7)	C5-C6	1.396 (9)
O1-C2	1.248 (9)	Re-C5	2.308 (6)	C6-C7	1.415 (10)
C1-C2	1.492 (12)	Re-C6	2.281 (6)	C7-C8	1.417 (11)
C2-C3	1.501 (12)	Re-C7	2.226 (8)	P1-C11	1.819 (7)
Re-P1	2.379 (2)	Re-C8	2.227 (8)	P1-C21	1.822 (6)
Re-N	1.758 (6)	C4-C5	1.398 (9)	P1-C31	1.838 (7)
N-O2	1.184 (8)	C4-C8	1.429 (9)		

N-Re-P1	92.6 (2)	O1-Re-C7	145.8 (2)
Re-N-O2	172.1 (5)	O1-Re-C8	136.2 (2)
O1-Re-N	103.8 (2)	C5-C4-C8	107.3 (6)
O1-Re-P1	84.1 (1)	C4-C5-C6	109.9 (6)
Re-O1-C2	136.3 (4)	C5-C6-C7	107.2 (6)
O1-C2-C1	118.6 (7)	C6-C7-C8	108.5 (6)
O1-C2-C3	122.5 (7)	C4-C8-C7	107.2 (6)
C1-C2-C3	118.9 (7)	Re-P1-C11	114.7 (2)
O1-Re-C4	99.8 (2)	Re-P1-C21	114.6 (2)
O1-Re-C5	87.9 (2)	Re-P1-C31	113.1 (2)
O1-Re-C6	110.0 (2)		

B. $3e^+PF_6^-$

Re-O1	2.080 (5)	C7-C8	1.382 (13)	C9-C10	1.404 (12)
O1-C2	1.245 (8)	Re-P1	2.397 (2)	C9-C13	1.418 (11)
C1-C2	1.494 (9)	Re-N	1.758 (5)	C10-C11	1.403 (13)
C2-C3	1.450 (10)	N-O2	1.199 (7)	C11-C12	1.356 (10)
C3-C4	1.388 (10)	Re-C9	2.224 (7)	C12-C13	1.428 (14)
C3-C8	1.391 (11)	Re-C10	2.278 (7)	P1-C21	1.835 (6)
C4-C5	1.399 (12)	Re-C11	2.336 (7)	P1-C31	1.827 (6)
C5-C6	1.377 (14)	Re-C12	2.310 (8)	P1-C41	1.829 (6)
C6-C7	1.350 (13)	Re-C13	2.229 (7)		

N-Re-P1	91.3 (2)	C3-C8-C7	120.9 (7)
Re-N-O2	171.4 (5)	O1-Re-C9	136.6 (2)
O1-Re-N	103.0 (2)	O1-Re-C10	100.7 (2)
O1-Re-P1	85.8 (1)	O1-Re-C11	87.8 (2)
Re-O1-C2	138.3 (4)	O1-Re-C12	108.1 (3)
O1-C2-C1	121.2 (6)	O1-Re-C13	144.1 (3)
O1-C2-C3	117.5 (5)	C10-C9-C13	105.9 (8)
C1-C2-C3	121.2 (6)	C9-C10-C11	108.4 (6)
C2-C3-C4	120.3 (7)	C10-C11-C12	110.0 (8)
C2-C3-C8	120.9 (6)	C11-C12-C13	106.9 (7)
C4-C3-C8	118.4 (7)	C9-C13-C12	108.7 (7)
C3-C4-C5	120.0 (8)	Re-P1-C21	113.6 (2)
C4-C5-C6	119.6 (8)	Re-P1-C31	112.4 (2)
C5-C6-C7	120.9 (9)	Re-P1-C41	117.6 (2)
C6-C7-C8	120.1 (9)		

C. (*RS,SR*)-**5e**

Re-O1	2.033 (4)	C7-C8	1.41 (1)	C9-C10	1.414 (9)
O1-C2	1.428 (7)	Re-N	1.744 (5)	C9-C13	1.39 (1)
C1-C2	1.518 (9)	N-O2	1.203 (6)	C10-C11	1.40 (1)
C2-C3	1.514 (8)	Re-P	2.356 (1)	C11-C12	1.42 (1)
C3-C4	1.386 (9)	Re-C9	2.282 (6)	C12-C13	1.39 (1)
C3-C8	1.379 (9)	Re-C10	2.228 (7)	P-C14	1.830 (6)
C4-C5	1.395 (9)	Re-C11	2.253 (7)	P-C20	1.837 (6)
C5-C6	1.38 (1)	Re-C12	2.337 (7)	P-C26	1.818 (6)
C6-C7	1.36 (1)	Re-C13	2.368 (7)		

N-Re-P	93.1 (2)	C4-C5-C6	118.8 (7)
Re-N-O2	176.6 (5)	C5-C6-C7	121.3 (7)
O1-Re-N	105.5 (2)	C6-C7-C8	119.6 (7)
O1-Re-P	80.0 (1)	C3-C8-C7	120.0 (7)
Re-O1-C2	118.8 (3)	C10-C9-C13	108.2 (7)
O1-C2-C1	110.5 (5)	C9-C10-C11	107.5 (7)
O1-C2-C3	107.5 (5)	C10-C11-C12	107.7 (7)
C1-C2-C3	112.2 (5)	C11-C12-C13	107.4 (7)
C2-C3-C4	120.7 (6)	C9-C13-C12	109.1 (7)
C2-C3-C8	119.8 (6)	Re-P-C14	117.0 (2)
C4-C3-C8	119.4 (6)	Re-P-C20	116.3 (2)
C3-C4-C5	120.8 (6)	Re-P-C26	110.5 (2)

P-Re-O-C2 and N-Re-O-C2 torsion angles were 158.0 (6)° and 67.5 (6)°, respectively.

The enantiomer of (*RS,SR*)-**5e** depicted in Figure 5 has an *R* configuration at rhenium and an *S* configuration at carbon, thus confirming the structures assigned to the major diastereomers in Schemes II and III. It is instructive to compare the bottom view of (*RS,SR*)-**5e** in Figure 5 with the bottom view of precursor $3e^+PF_6^-$ in Figure 3. The observed stereochemistry is clearly consistent with hydride attack upon the acetophenone ligand carbonyl carbon from a direction anti to the bulky PPh_3 ligand.

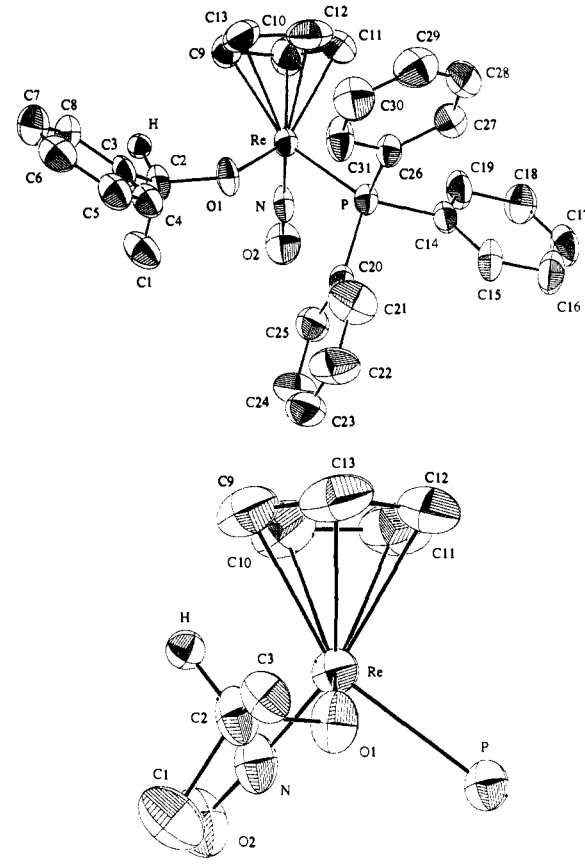

Figure 5. Views of the alkoxide complex (*RS,SR*)-(η^5-C_5H_5)Re(NO)(PPh_3)($OCH(CH_3)C_6H_5$) ((*RS,SR*)-**5e**). Top: Numbering diagram. Bottom: View down the oxygen-rhenium bond with phenyl rings omitted.

6. Synthesis of Optically Active Ketone and Alkoxide Complexes. Optically active ketone complexes (+)-(*R*)-**3a**-$e^+BF_4^-$ and (+)-(*R*)-**3a,b,e**$^+PF_6^-$ were prepared from optically active methyl complex (+)-(*S*)-**1** by procedures similar to those given above for the racemates.[27] The enantiomer (−)-(*S*)-$\mathbf{3d}^+BF_4^+$ was also prepared from (−)-(*R*)-**1** for control experiments. The optically active ketone complexes were distinctly less crystalline than the racemates, and readily oiled. Analytically pure powders could be obtained, but usually with difficulty. In some cases, better yields and/or purities were obtained when (+)-(*S*)-**1**, $HBF_4{\cdot}O(C_2H_5)_2$, and ketones were reacted in chlorobenzene (Experimental Section). Under these conditions, chlorobenzene complex [(η^5-C_5H_5)Re(NO)(PPh_3)(ClC_6H_5)]$^+BF_4^-$ is generated.[31]

Complexes (+)-(*R*)-$\mathbf{3}^+X^-$ were characterized by optical rotations,[30] and their spectroscopic properties closely matched those of the racemates. Absolute configurations, corresponding to retention at rhenium, were assigned by analogy to other substitution reactions of dichloromethane complex $\mathbf{2}^+X^-$.[12,31] Further, as noted previously for this class of compounds, the sign of the optical rotation at 589 nm nearly always correlates with the absolute configuration.[9a,c,10,12,22,24,31,32]

The chiral NMR shift reagent (+)-Eu(hfc)$_3$ (2.5 equiv, CD_2Cl_2) effected near-baseline resolution of the cyclopentadienyl ^1H NMR resonances of the enantiomers of racemic acetone complex $\mathbf{3a}^+$-

(30) (a) All [α] were measured in thermostated cells (25.0 ± 0.2 °C) in $CHCl_3$ with *c* in the range of 0.9–1.2 g/mL. (b) If optically active $\mathbf{3}^+BF_4^-$ and $\mathbf{3}^+PF_6^-$ behave ideally in solution, [α] for the former should be 7–9% greater, as the observed rotation α is divided by g/mL (as opposed to mol/mL). Due to the supplier problems noted above,[15] we were unable to make replicate determinations of [α] for $\mathbf{3}^+PF_6^-$.

(31) Kowalczyk, J. J.; Agbossou, S. K.; Gladysz, J. A. *J. Organomet. Chem.* In press.

BF_4^-. Identical analysis of (+)-(*R*)-**3a**$^+BF_4^-$ showed no trace of the other enantiomer. Reactions described below also place high boundary limits on the optical purities of (+)-(*R*)-**3**$^+BF_4^-$.

We sought to assay the configurational stabilities of (+)-(*R*)-**3**$^+BF_4^-$. Thus, CH_2Cl_2 and CD_2Cl_2 solutions of acetone complex (+)-(*R*)-**3a**$^+BF_4^-$ were kept at 25 °C and monitored polarimetrically and by ^{1}H NMR. Over the course of 24 h, considerable decomposition occurred. Shift reagent analysis showed the remaining (+)-(*R*)-**3a**$^+BF_4^-$ (30–40%) to be 58% ee. The observed rotations α indicated that at least some of the decomposition products were optically active.

Optically active ketone complexes (+)-(*R*)-**3a–e**$^+BF_4^-$ and K(*sec*-$C_4H_9)_3BH$ were reacted as described for the racemates above. The resulting optically active alkoxide complexes (+)-(*RS*)-**5a–e** showed a marked tendency to oil but were ultimately isolated as powders in 54–92% yields (Scheme II, entries 7–10). Diastereomeric excesses were similar to those obtained with the racemates.[28] Complexes (+)-(*RS*)-**5a–e** were characterized (as mixtures of diastereomers) by microanalyses and optical rotations (Experimental Section). The stereochemistry at rhenium (retention) was assigned by analogy to that observed for a variety of reactions involving nucleophilic attack upon coordinated ligands.[9a,e,32,33] This was supported by the signs of the optical rotations and reactions described below.

Reactions of optically active ketone complexes and formyl complex **7** were examined. First, (+)-(*R*)-**3b,e**$^+BF_4^-$ were treated with *racemic* **7** (Scheme III, entries 3 and 4). Alkoxide complexes (+)-**5b,e** formed as 90.5:9.5 and 98.0:2.0 mixtures of (*RS*)/(*RR*) diastereomers,[28] respectively. Next, we sought to determine whether enantiomers of **7** might exhibit different stereoselectivities. In connection with another study, deuterioformyl complex (η^5-C_5H_5)Re(NO)(PPh_3)(CDO) (**7**-d_1) had been isolated in optically active form.[10c] As shown in entry 5 of Scheme III, reaction of (+)-(*R*)-**3b**$^+BF_4^-$ and (+)-(*S*)-**7**-d_1 gave (+)-**5b**-d_1 as a 97.5:2.5 mixture of (*RS*)/(*RR*) diastereomers—a ratio considerably higher than in entries 1 and 3. An analogous reaction of (+)-(*R*)-**3b**$^+BF_4^-$ and (−)-(*R*)-**7**-d_1 (entry 6) gave (+)-**5b**-d_1 as a 83.0:17.0 mixture of diastereomers. Thus, one enantiomer of **7** reduces a given enantiomer of ketone complex **3**$^+BF_4^-$ with considerably higher stereoselectivity than the other enantiomer of **7**.

7. Conversion of Alkoxide Complexes to Organic Compounds. We sought to (1) provide further support for the configurations assigned to diastereomeric alkoxide complexes **5b–e**, (2) elaborate the alkoxide ligands to optically active organic compounds, and (3) demonstrate means by which the chiral rhenium auxiliary might be recycled. Importantly, optically active "Mosher esters", $C_6H_5(CH_3O)(F_3C)CC(=O)OCH(CH_3)R$ (**10b–e**, MTPA-$OCH(CH_3)R$), corresponding to each of the alkoxide complexes have been previously prepared.[34] Absolute configurations have in all cases been unambiguously assigned.

Primary alkoxide complexes (η^5-C_5H_5)Re(NO)(PPh_3)(OCH_2R) and acyl halides (R′COX) readily react at room temperature to give esters $R'CO_2CH_2R$ and halide complexes (η^5-C_5H_5)Re(NO)(PPh_3)(X).[10] Thus, racemic alkoxide complexes **5b–e**, the optically active "Mosher acid chloride" (+)-(*S*)-MTPA-Cl, and the base 4-(dimethylamino)pyridine (DMAP) were combined in benzene at 50 °C (Scheme II). Chromatographic workup gave esters **10b–e** in 80–98% yields as equal mixtures of (*RS*)/(*RR*) diastereomers.

Scheme V. Conversion of Optically Active Alkoxide Complexes to Optically Active Rhenium Complexes; Representative Methods for Recycling the Chiral Auxiliary

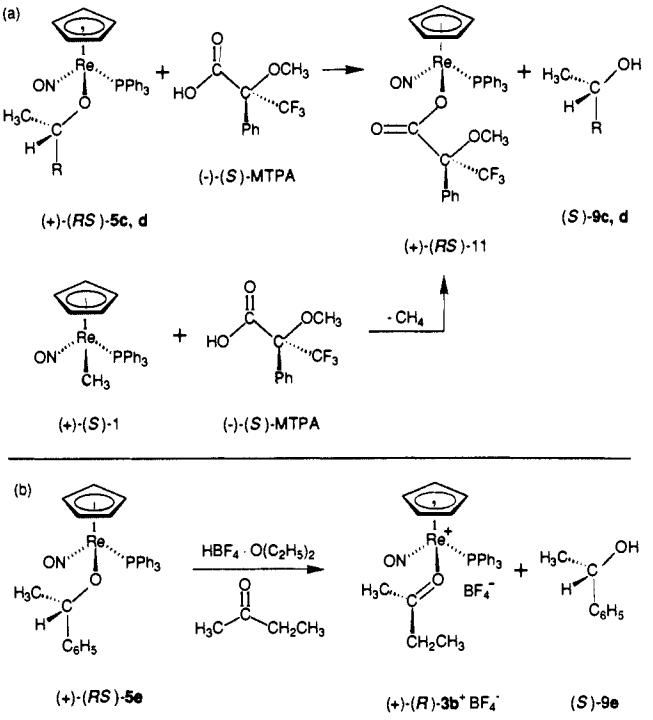

Next, optically active alkoxide complexes (+)-(*RS*)-**5b,c** were reacted similarly. Workup gave esters (*RS*)-**10b,c** in 99% and 97% yields, and de of 79% and 93%, respectively (Scheme II). Diastereomeric excesses were assayed by NMR and/or GLC[34c] and closely matched those of the precursor alkoxide complexes (+)-(*RS*)-**5b,c**. The previously established ester configurations[34a] confirm the configurations assigned to the alkoxide ligand carbons of (+)-(*RS*)-**5b,c**.

Analogous reactions of (+)-(*RS*)-**5d,e** gave esters (*RS*)-**10d,e** in diastereomeric excesses that were slightly lower than those of (+)-(*RS*)-**5d,e**. Control experiments showed that the alkoxide complexes underwent slow epimerization at carbon at 50 °C.[36] Thus, the preceding cleavage reactions were repeated at room temperature (12–16 h), followed by a brief period at 50 °C. This gave (*RS*)-**10d,e** in 98–96% de (Scheme II).

The rhenium-containing byproduct in the preceding reactions, chloride complex (η^5-C_5H_5)Re(NO)(PPh_3)(Cl) (**6**), is easily isolated in high yield.[35] However, **6** is not very configurationally stable.[24] Hence, we sought means of alkoxide ligand detachment that would give a rhenium complex that could be isolated in optically active form.

Accordingly, (+)-(*RS*)-**5c,d** were treated with Mosher's acid, (−)-(*S*)-MTPA (1.0 equiv, C_6D_6, room temperature; Scheme Va). Alcohols (*S*)-**9c,d** were detected by ^{1}H NMR but were not directly assayed for optical purity.[37] Carboxylate complex (+)-(*RS*)-(η^5-C_5H_5)Re(NO)(PPh_3)(OC(=O)C(CF_3)(OCH_3)C_6H_5) ((+)-(*RS*)-**11**) formed in ≥99% de, as assayed by integration of the cyclopentadienyl ^{1}H NMR resonances. Workup gave (+)-(*RS*)-**11** in 92–93% yields.

Optically active methyl complex (+)-(*S*)-**1** has been previously shown to react with acids HX to give complexes (η^5-C_5H_5)Re(NO)(PPh_3)(X) with *retention* of configuration at rhenium.[10,24]

(32) Merrifield, J. H.; Lin, G.-Y.; Kiel, W. A.; Gladysz, J. A. *J. Am. Chem. Soc.* **1983**, *105*, 5811.

(33) (a) Brunner, H. *Adv. Organomet. Chem.* **1980**, *18*, 151. (b) Flood, T. C.; Campbell, K. D.; Downs, H. H.; Nakanishi, S. *Organometallics* **1983**, *2*, 1590. (c) Faller, J. W.; Chao, K.-H. *Ibid.* **1984**, *3*, 927. (d) Consiglio, G.; Morandini, F. *Chem. Rev.* **1987**, *87*, 761.

(34) (a) Dale, J. A.; Dull, D. L.; Mosher, H. S. *J. Org. Chem.* **1969**, *34*, 2543. (b) The ester (*RS*)-**10e** was prepared earlier but its configuration was not assigned.[34a] We confirmed the assignment in Scheme II by synthesis of an authentic sample from (+)-(*R*)-MTPA, (−)-(*S*)-1-phenylethanol, and standard reagents:[35] Neises, B.; Steglich, W. *Angew. Chem., Int. Ed. Engl.* **1978**, *17*, 522. (c) Diastereomer ratios were determined by ^{1}H NMR (**10b**: $OCCH_3$, CH_2CH_3; **10c**: $OCHCH_3$, OCH_3; **10d**: $C(CH_3)_3$) and GLC (**10c–e**).[5d,6c] The NMR and GLC values agreed within 0.5% (**10c,d**).

(35) Dalton, D. M. Ph.D. Thesis, University of Utah, 1990.

(36) A C_6D_6 solution of (+)-(*RS*)-**5d** (99% de) was kept at 53 °C for 9.5 h. The sample was treated with CF_3CO_2H to generate alcohol **9d**. Subsequent addition of (+)-(*S*)-MTPACl/DMAP gave ester (*RS*)-**10d** of 67% de. Hence, epimerization occurs at *carbon*. However, analogous amide complexes have been shown to undergo epimerization at rhenium at similar temperatures: Dewey, M. A.; Gladysz, J. A. *Organometallics* **1990**, *9*, 1317.

(37) Complexes (+)-(*RS*)-**5d,e** were also treated with HCl at −80 °C. The resulting alcohols were reacted with (+)-(*S*)-MTPACl/DMAP. Esters (*RS*)-**10d,e** were isolated in diastereomeric excesses that matched those of (+)-(*RS*)-**5d,e**.

Chart II. Structurally Characterized Acetone Complexes (**12–15**) and Related σ Complexes (**16** and **17**)

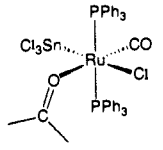

12

C=O 1.238(9) Å
Ru-O-C 153.0(5)°

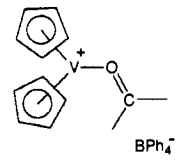

13

C=O 1.223(5) Å
V-O-C 136.8(4)°

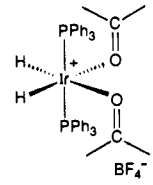

14

C=O 1.216(8) Å
C=O 1.242(8) Å
Ir-O-C 133.1(5)°
Ir-O-C 134.9(6)°

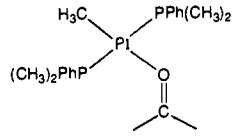

15

C=O 1.225(7) Å
Pt-O-C 129.4(4)°

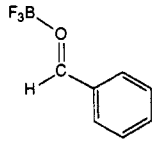

16

C=O 1.244(5) Å
B-O-C 118.7(3)°

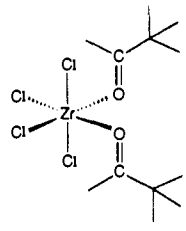

17

C=O 1.246(3) Å
C=O 1.250(3) Å
Zr-O-C 153.2(2)°
Zr-O-C 148.2(2)°

Hence, an authentic sample of (+)-(*RS*)-**11** was prepared by reaction of (+)-(*S*)-**1** and (−)-(*S*)-MTPA (Scheme Va). An authentic sample of the opposite diastereomer, (+)-(*RR*)-**11**, was similarly prepared from (+)-(*S*)-**1** and (+)-(*R*)-MTPA. Each diastereomer exhibited distinctive ^{1}H NMR resonances and was characterized analogously to the other new optically active compounds (Experimental Section).

Finally, we sought to recycle the rhenium auxiliary to a ketone complex. Accordingly, optically active 1-phenylethoxide complex (+)-(*RS*)-**5e** was treated with $HBF_4{\cdot}O(C_2H_5)_2$ (1.0 equiv) in dichloromethane at −80 °C (Scheme Vb). Then excess 2-butanone was added. Subsequent GC analysis showed the presence of 1-phenylethanol (**9e**, 71%). Workup gave 2-butanone complex (+)-(*RS*)-**3b**$^+BF_4^-$ in 78% yield and 93% ee.[38]

Discussion

1. Structures of Ketone Complexes. Although a variety of σ and π ketone complexes have been reported in the literature,[3,39]

Scheme VI. Possible Mechanisms for Intramolecular Exchange of *E* and *Z* Methyl Groups in Acetone Complex **3a**$^+BF_4^-$

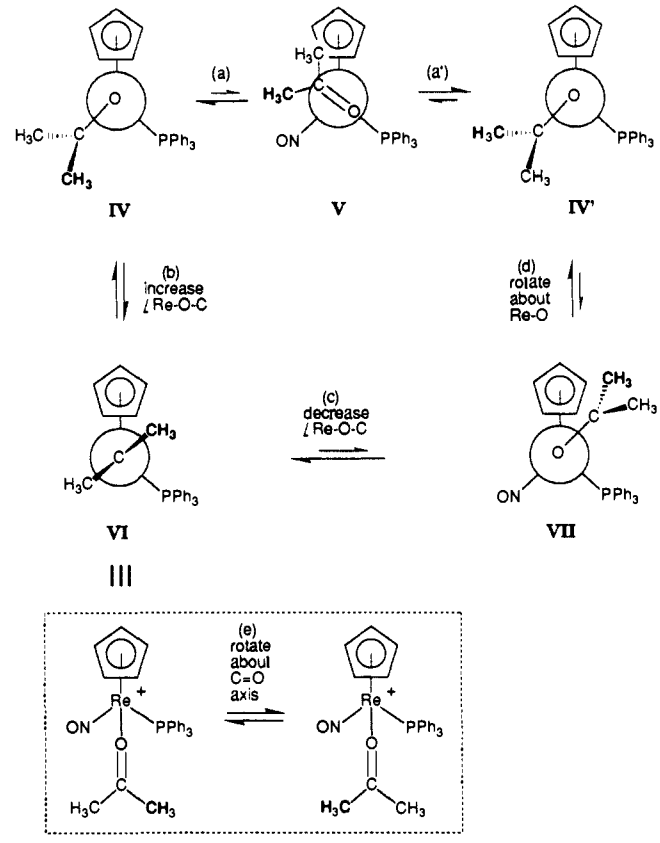

little attention has been given to the factors that influence the relative energies of the σ and π coordination modes.[39a] As noted above, ketones and aliphatic aldehydes exhibit contrasting ground-state binding behavior toward the rhenium fragment $[(\eta^5\text{-}C_5H_5)Re(NO)(PPh_3)]^+$ (**I**). We have previously attributed this dichotomy to (1) the greater bulk of ketones, which disfavors π binding, and (2) the greater π acidity of aldehydes,[23] which favors π binding. However, the σ and π coordination modes can be comparable in energy in analogous *aromatic* aldehyde complexes.[16]

The crystal structures of **3a**,**e**$^+PF_6^-$ (Figures 2 and 3) provide starting points for analyzing the highly stereoselective reductions in Schemes II and III. First, both compounds exhibit essentially coplanar five-atom Re—O=C(C)$_2$ linkages that nearly eclipse the Re-NO bond. The C=O bonds (1.248 (9), 1.245 (8) Å) appear slightly longer than those of free acetone (1.222 (3) Å)[40] and acetophenone (1.216 (2) Å).[41] This is an expected consequence of the σ donor interaction and π backbonding from the d orbital shown in **I** (Chart I) to the C=O π^* orbital.[42]

A search of the Cambridge crystallographic data base located four structurally characterized σ acetone complexes that were related to **3a**$^+PF_6^-$ (**12–15**, Chart II).[43] No crystal structures of σ-acetophenone complexes were found.[44] Acetone complexes

(38) This experiment was designed to give an alcohol that could easily be assayed by GC. However, since the optically active acetophenone complex (+)-(*RS*)-**3e**$^+BF_4^-$ is difficult to isolate, 2-butanone was employed as the trapping ketone.

(39) Some key papers on transition-metal–ketone complexes that have appeared since the publication of ref 3: (a) Harman, W. D.; Sekine, M.; Taube, H. *J. Am. Chem. Soc.* **1988**, *110*, 2439. (b) Harman, W. D.; Dobson, J. C.; Taube, H. *Ibid.* **1989**, *111*, 3061. (c) Müller, J.; Hänsch, C.; Pickardt, J. *Z. Naturforsch.* **1989**, *44b*, 278. (d) Covert, K. J.; Wolczanski, P. T. *Inorg. Chem.* **1989**, *28*, 4565. (e) Galeffi, B.; Simard, M.; Wuest, J. D. *Ibid.* **1990**, *29*, 951. (f) Bryan, J. C.; Mayer, J. M. *J. Am. Chem. Soc.* **1990**, *112*, 2298. (g) Chisholm, M. H.; Folting, K.; Klang, J. A. *Organometallics* **1990**, *9*, 607. (h) Shambayati, S.; Crowe, W. E.; Schreiber, S. L. *Angew. Chem., Int. Ed. Engl.* **1990**, *29*, 256.

(40) Nelson, R.; Pierce, L. *J. Mol. Spectrosc.* **1965**, *18*, 344.

(41) Tanimoto, Y.; Kobayashi, H.; Nagakura, S.; Saito, Y. *Acta Crystallogr.* **1973**, *B29*, 1822.

(42) This bond lengthening is more pronounced in the crystal structure of the σ aromatic aldehyde complex $[(\eta^5\text{-}C_5H_5)Re(NO)(PPh_3)(\eta^1\text{-}O{=}CH\text{-}p\text{-}C_6H_4OCH_3)]^+PF_6^-$(C=O, 1.271 (8) Å).[16b]

(43) (a) Gould, R. O.; Sime, W. J.; Stephenson, T. A. *J. Chem. Soc., Dalton Trans.* **1978**, 76. (b) Gambarotta, S.; Pasquali, M.; Floriani, C.; Chiesi-Villa, A. *Inorg. Chem.* **1981**, *20*, 1173. (c) Crabtree, R. H.; Hlatky, G. G.; Parnell, C. P.; Segmüller, B. E.; Uriarte, R. J. *Ibid.* **1984**, *23*, 354. (d) Thayer, A. G.; Payne, N. C. *Acta Crystallogr.* **1986**, *C42*, 1302.

(44) However, several σ complexes of related ketones were located: (a) Knobler, C. B.; Crawford, S. S.; Kaesz, H. D. *Inorg. Chem.* **1975**, *14*, 2062. (b) McGuiggan, M. F.; Pignolet, L. H. *Ibid.* **1982**, *21*, 2523. (c) Crist, D. R.; Hseih, Z.-H.; Quicksall, C. O.; Sun, M. K. *J. Org. Chem.* **1984**, *49*, 2478. (d) van Koningsveld, H.; Scheele, J. J.; Jansen, J. C. *Acta Crystallogr.* **1986**, *C42*, 41.

12–15 exhibit C=O bond lengths that range from 1.216 (8) to 1.242 (8) Å, with an average of 1.229 Å. The slightly longer C=O bond in $\mathbf{3a}^+PF_6^-$ likely reflects the greater π basicity of the rhenium fragment $[(\eta^5\text{-}C_5H_5)Re(NO)(PPh_3)]^+$. Interestingly, the formaldehyde analogue of vanadium acetone complex **12** has also been structurally characterized, and in accord with the generalizations given above it exhibits a π-binding mode.[45]

The Re–O–C angles in $\mathbf{3a,e}^+PF_6^-$ (136.3 (4)°, 138.3 (4)°) are somewhat greater than would be expected from a bonding model involving sp^2-hybridized oxygen. This feature is found in nearly all σ ketone and aldehyde complexes of transition metals. For example, acetone complexes **12–15** exhibit M–O–C angles that range from 129.4 (4)° to 153.0 (5)°, with an average of 137.4°. In some cases, donation from an occupied orbital on oxygen to a metal acceptor orbital has been proposed.[39e] Accordingly, the σ complex of BF_3 (which lacks low-lying acceptor orbitals) and benzaldehyde exhibits a B–O–C bond angle of only 118.7 (3)° (**16**, Scheme VI).[46]

Coordinatively saturated complexes of the formula $(\eta^5\text{-}C_5H_5)MLL'L''$ are formally octahedral. Thus, L–Re–N and L–Re–P bond angles of ca. 90° are commonly found in $[(\eta^5\text{-}C_5H_5)Re(NO)(PPh_3)(L)]^{n+}$ complexes.[8,9b,c,20–22] However, $\mathbf{3a,e}^+PF_6^-$ show significant distortions (∠O–Re–N = 103.8 (2)°, 103.0 (2)°; ∠O–Re–P = 84.1 (1)°, 85.8 (1)°). In order to compare this feature in different complexes (see below), we sum the deviation of the two angles from 90°. This gives 19.7° for $\mathbf{3a}^+PF_6^-$ and 17.2° for $\mathbf{3e}^+PF_6^-$.

2. Dynamic Equilibria in Ketone Complexes. Potential equilibria in solution must also be considered before interpreting the reductions in Schemes II and III. Figure 1 and other data establish a rapid intramolecular pathway for methyl group exchange in acetone complex $\mathbf{3a}^+BF_4^-$. Two limiting mechanisms can be envisioned, as sketched for degenerate structures IV and IV′ in Scheme VI.

First, a π-acetone complex might initially form (V; step a). Intermediate V is shown in a Re–(C⌣O) conformation analogous to that found in the corresponding π aldehyde complexes $\mathbf{4}^+X^-$.[10] This isomerization requires rotation about both the Re—O bond and C=O axis of IV. The π complex can return to a σ complex via either a counterclockwise rotation about the C⌣O axis, which gives starting isomer IV, or a clockwise rotation, which gives exchanged isomer IV′ (step a′).

Our IR and NMR data indicate that π isomers of $\mathbf{3}^+X^-$ are at least 2 kcal/mol higher in energy than the ground state σ isomers. However, $\Delta G^{\ddagger}_{133K}$ for the interconversion of IV and IV′ is only 6 kcal/mol. This imposes an upper limit of 4 kcal/mol on $\Delta G^{\ddagger}$ for the isomerization of V to IV′ (or IV). This barrier seems implausibly low for a process that involves coupled rotational motions in a sterically congested environment. Hence, we disfavor this mechanism.

Other mechanistic possibilities for methyl group exchange in $\mathbf{3a}^+BF_4^-$ involve opening the Re–O–C bond of IV to the "linear" σ intermediate or transition state VI (step b, Scheme VI). Continuation of this reaction coordinate (step c) would give the Re–O rotamer VII, and a 180° Re–O bond rotation (step d; perhaps rate determining) would be required to complete the exchange. Alternatively, rotation could occur about the C=O axis at any point connecting IV and VI, as illustrated in step e. Reversal of the reaction coordinate would then give IV′.

There have been several theoretical studies of complexes of aldehydes and ketones with main group Lewis acids such as BF_3, $AlCl_3$, and Li^+.[46,47] With BF_3 and $AlCl_3$, bent σ complexes are found to be energy minima, and linear σ complexes are found to be energy maxima. However, the linear complexes are the lowest energy transition states for alkyl group exchange and are only a few kcal/mol less stable than the bent complexes. A linear ground state is found for Li^+—O=CH_2,[47a] and crystal structures of alkali metal/ketone adducts show both linear and bent M^+—O=CRR′ linkages.[39h,48] Accordingly, we favor mechanisms involving the linear species VI for methyl group exchange in $\mathbf{3a}^+BF_4^-$.

Scheme VII. Some Relevant Equilibria of Ketone Derivatives

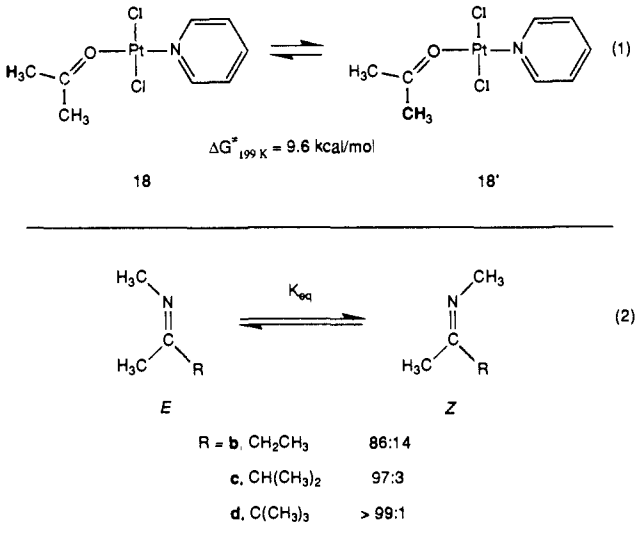

The rapid intramolecular exchange of alkyl groups in σ ketone complexes has precedent. Courtot has been able to decoalesce the methyl ^1H and ^{13}C NMR resonances in the platinum acetone complex *trans*-$Cl_2Pt(pyr)(\eta^1\text{-}O{=}C(CH_3)_2)$ (**18**; Scheme VII).[49] His data give $\Delta G^{\ddagger}_{199K}$ of ca. 9.6 kcal/mol. Control experiments show exchange with *free* acetone-d_6 to be slow. Wuest finds methyl group exchange in the zirconium bis(acetone) complex $Cl_4Zr(\eta^1\text{-}O{=}C(CH_3)_2)_2$ to be rapid on the NMR time scale at −120 °C.[39e] Both investigators have proposed mechanisms involving linear σ complexes. We predict that such facile dynamic equilibria will prove to be general for transition-metal σ-ketone complexes.[50]

3. Geometric Isomerism in Ketone Complexes. In view of the low barrier for methyl group exchange in $\mathbf{3a}^+BF_4^-$, *E*/*Z* C=O geometric isomers of unsymmetrical ketone complexes $\mathbf{3b\text{–}e}^+X^-$ should rapidly equilibrate in solution. Thus, both isomers should be available on the time scale of the reductions in Schemes II and III.

To our knowledge, no *E*/*Z* equilibrium constants have been determined for metal complexes of unsymmetrical ketones. In particular, the platinum 2-butanone complex *trans*-$Cl_2Pt(pyr)(\eta^1\text{-}O{=}C(CH_3)CH_2CH_3)$ has been studied by low-temperature NMR.[49] No decoalesence of *E*/*Z* isomers was observed under conditions where the analogous acetone complex (**18**, Scheme VII) gave distinct *E*/*Z* methyl ^1H and ^{13}C NMR resonances.[50] However, *E* C=O geometric isomers are commonly found in the crystal structures of methyl ketone complexes.[39e,44c,d] For example, the zirconium is cis to the methyl group in bis(3,3-dimethyl-2-butanone) complex $Cl_4Zr(\eta^1\text{-}O{=}C(CH_3)C(CH_3)_3)_2$ (**17**, Chart II).[39e]

(45) Gambarotta, S.; Floriani, C.; Chiesi-Villa, A.; Guastini, C. *Organometallics* **1986**, *5*, 2425.
(46) Reetz, M. T.; Hüllmann, M.; Massa, W.; Berger, S.; Rademacher, P.; Heymanns, P. *J. Am. Chem. Soc.* **1986**, *108*, 2405.
(47) (a) Raber, D. J.; Raber, N. K.; Chandrasekhar, J.; Schleyer, P. v. R. *Inorg. Chem.* **1984**, *23*, 4076. (b) Nelson, D. J. *J. Org. Chem.* **1986**, *51*, 3185. (c) LePage, T. J.; Wiberg, K. B. *J. Am. Chem. Soc.* **1988**, *110*, 6642.
(48) (a) Willard, P. G.; Carpenter, G. B. *J. Am. Chem. Soc.* **1986**, *108*, 462; see compound **3**. (b) Engelhardt, L. M.; Harrowfield, J. M.; Lappert, M. F.; MacKinnon, I. A.; Newton, B. H.; Raston, C. L.; Skelton, B. W.; White, A. H. *J. Chem. Soc., Chem. Commun.* **1986**, 846. (c) Amstutz, R.; Dunitz, J. D.; Laube, T.; Schweizer, W. B.; Seebach, D. *Chem. Ber.* **1986**, *119*, 434.
(49) (a) Courtot, P.; Pichon, R.; Salaun, J. Y. *J. Organomet. Chem.* **1985**, *286*, C17. (b) Auffret, J.; Courtot, P.; Pichon, R.; Salaün, J.-Y. *J. Chem. Soc., Dalton Trans.* **1987**, 1687.
(50) Data on ketone–BF_3 complexes are similar. For example, the barrier to intramolecular ethyl group exchange in the 3-pentanone complex F_3B—O=$C(CH_2CH_3)_2$ has been determined by ^{13}C NMR ($\Delta G^{\ddagger}_{172K}$ = 8.3 kcal/mol). However, methyl group exchange in the acetone complex F_3BO=$C(CH_3)_2$ was rapid on the NMR time scale at −110 °C. Similarly, the *E*/*Z* geometric isomers of the 2-butanone complex F_3B—O=$C(CH_3)CH_2CH_3$ could not be decoalesced, although chemical shift data indicated that the *E* isomer predominated: Hartman, J. S.; Stilbs, P.; Forsén, S. *Tetrahedron Lett.* **1975**, *16*, 3497.

Table IV. Comparison of Hydride-Based Methods for the Asymmetric Reduction of 2-Butanone

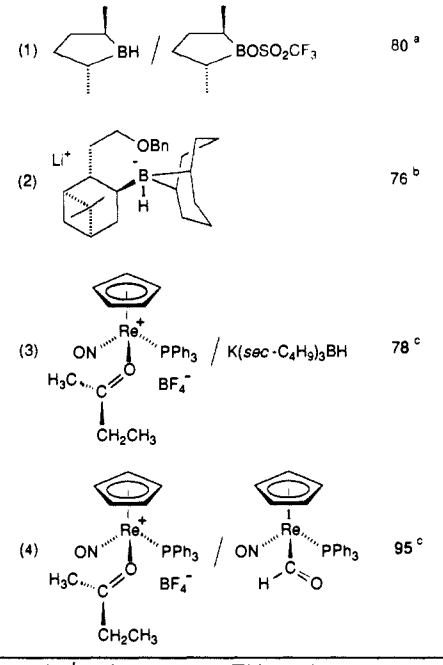

[a] Reference 5d. [b] Reference 5b. [c] This study.

Equilibrium constants have been determined for E/Z C=N geometric isomers of *imines* of methyl ketones.[51] Data for 2-butanone, 3-methyl-2-butanone, and 3,3-dimethyl-2-butanone derivatives are given in Scheme VII. The K_{eq} show E isomers to be greatly favored and exhibit the expected trend as the size of the non-methyl substituent is increased. The E C=O isomer of the σ complex of 2-butanone and BF_3 also greatly predominates in solution.[50] Hence, we assume that E/Z isomers of **3b–e**$^+$X$^-$ exhibit similar K_{eq} values and trends. Note that the reduction stereoselectivities in Scheme II parallel the E/Z ratios in Scheme VII.

4. Transition States and Stereoselectivities of Ketone Ligand Reduction. It has been shown that the σ complexation of aldehydes by BF_3 lowers the energies of the C=O π^* orbitals and increases the magnitudes of the coefficients at carbon.[46] Both effects enhance the rate of nucleophilic addition. We presume that similar reactivity-enhancing effects are operative in **3**$^+$X$^-$, as evidenced by the C=O bond length trends noted above. As exemplified elsewhere,[10c] the dominant reduction stereochemistry in Schemes II and III can also be rationalized by nucleophilic attack upon π isomers of **3**$^+$X$^-$. However, we are unable to identify any factor that would render a π mechanism energetically more favorable.

Since two diastereomers of alkoxide complexes **5** are produced upon reduction of **3b–e**$^+$X$^-$, at least two transition states must be operative. As noted above, the dominant stereochemistry is consistent with hydride attack upon σ isomer E-II from a direction anti to the PPh_3 ligand. We prefer to view the minor diastereomers of **5** as arising by analogous attack upon the geometric isomer Z-II (Chart I). However, hydride attack on rotamer E-III could also give the minor diastereomers. Both Z-II and E-III orient the opposite ketone enantioface anti to the PPh_3 ligand.[52]

Several optically active hydride reagents are available that reduce acetophenone to 1-phenylethanol of ≥98% ee.[5a-g,6c-e] However, the best previously reported methods for the asymmetric reduction of 2-butanone give 2-butanol of only about 80% ee.[5b,d,f] These are summarized in Table IV. This drop can be attributed to the decrease in size difference of the carbonyl substituents—a factor that impacts relative E/Z binding rates and energies, as well as energies of hydride transfer transition states.

The racemic formyl complex **7** reduces 2-butanone and acetophenone complexes **3b,e**$^+$$BF_4^-$ with stereoselectivities that are comparable to K(*sec*-$C_4H_9)_3BH$.[53] However, **7** can be obtained in optically active form, and optically active 2-butanone complex (+)-(*R*)-**3b**$^+$$BF_4^-$ is reduced with considerably higher stereoselectivity by one enantiomer than the other (Scheme III). There is abundant precedent for this effect in reactions of two optically active compounds, and the term "double asymmetric induction" is often applied.[54] Thus, the combination of a chiral, optically active binding agent and a chiral, optically active hydride donor allows the reduction of 2-butanone to 2-butanol in optical yields (95% ee) that are considerably higher than those obtained by any other presently known method.

We have found analogous "double asymmetric induction" in reactions of **7** and π aldehyde complexes **4**$^+$$BF_4^-$,[10c] and stereoselectivity enhancements were documented in six substrates. Thus, this phenomenon has considerable generality and suggests a common reduction mechanism for the two classes of substrates. Note that each enantiomer of **7** would have distinct rate constants, k_E and k_Z, for the reduction of geometric isomers E-II and Z-II. Thus, a possible rationale of this effect is that one enantiomer of **7** has a higher k_E/k_Z ratio than the other. We presume a Dunitz trajectory.[55] but otherwise little is known regarding transition states for hydride transfer from formyl complexes.

5. Extensions. The diastereoselective addition of nucleophiles to **3b–e**$^+$X$^-$ and related complexes appears to have considerable generality. For example, **3b–e**$^+$X$^-$ are attacked with similar stereoselectivity by cyanide and acetylide ions.[10a,56] The resulting tertiary alkoxide complexes are configurationally stable and easily isolated. Analogous imine-type complexes also undergo stereoselective nucleophile addition.[11] However, it is probable that complexes of ketones where the two alkyl groups are not sterically differentiated, i.e., large/small as **3b–e**$^+$X$^-$, will not show high addition stereoselectivities.

The addition products, alkoxide complexes **5**, are versatile intermediates. The oxygens in primary alkoxide complexes (η^5-C_5H_5)Re(NO)(PPh_3)(OCH_2R) have been shown to be much more basic and nucleophilic than those of analogous ethers.[29,57] Consequently, reactions readily occur with protonating, alkylating, silylating, and acylating agents of the general formula E$^+$X$^-$.[10c,29,57] Organic derivatives $EOCH_2R$ and rhenium complexes (η^5-C_5H_5)Re(NO)(PPh_3)(X) are subsequently isolated in high yields. Configuration is frequently retained in the rhenium product. However, steric effects are sometimes noticeable. For example, secondary alkoxide complexes are less reactive than primary alkoxide complexes, and bulkier electrophiles attack more slowly.

Several unusual properties of alkoxide complexes **5** are receiving ongoing study. For example, the carbon-based epimerization[36] that occurs slightly above room temperature has been developed into a catalytic method for alcohol epimerization.[58] However, little is presently known about the mechanism. Interestingly, analogous amide complexes (η^5-C_5H_5)Re(NO)(PPh_3)(HNCHRR') epimerize at *rhenium* above room temperature.[59] Also, the N–Re–O and P–Re–O bond angles in the crystal structure of 1-phenylethoxide complex (*RS,SR*)-**5e** (105.5 (2)°,

(51) McCarty, C. G. In *The Chemistry of the Carbon–Nitrogen Double Bond*; Patai, S., Ed.; Wiley: New York, 1970; p 376.

(52) Vinyl complexes (η^5-C_5H_5)Re(NO)(PPh_3)(CH=CHR) can be considered "isosteric" with **3**$^+$X$^-$, and undergo *electrophilic* attack at C_β.[9b] Interestingly, rotamers that are analogous to E-II and E-III are *both* reactive (ca. 90:10).

(53) Note that K(*sec*-$C_4H_9)_3BH$ contains three asymmetric carbons and can exist as two diastereomers, both of which are chiral. Thus, there is potential for nonlinear stereoselectivity effects and related phenomena with reductions by this reagent. See: (a) Wynberg, H.; Feringa, B. *Tetrahedron* **1976**, *32*, 2831. (b) Puchot, C.; Samuel, O.; Duñach, E.; Zhao, S.; Agami, C.; Kagan, H. B. *J. Am. Chem. Soc.* **1986**, *108*, 2353.

(54) (a) Masamune, S.; Choy, W.; Peterson, J. S.; Sita, L. R. *Angew. Chem., Int. Ed. Engl.* **1985**, *24*, 1. (b) Nakayama, K. *J. Chem. Educ.* **1990**, *67*, 20. (c) Roush, W. R.; Hoong, L. K.; Palmer, M. A. J.; Straub, J. A.; Palkowitz, A. D. *J. Org. Chem.* **1990**, *55*, 4117.

(55) Bürgi, H. B.; Dunitz, J. D. *Acc. Chem. Res.* **1983**, *16*, 153.

(56) Dalton, D. M.; Gladysz, J. A. Manuscript in preparation.[35]

(57) Agbossou, S. K.; Fernández, J. M.; Gladysz, J. A. *Inorg. Chem.* **1990**, *29*, 476.

(58) Saura-Llamas, I.; Garner, C. M.; Gladysz, J. A. Manuscript in preparation.

(59) Dewey, M. A.; Gladysz, J. A. *Organometallics* **1990**, *9*, 1351.

80.0 (1)°) exhibit the most pronounced distortion from idealized octahedral geometry observed in these compounds to date (total deviation from 90° = 25.5°). These deformations may hold an important clue about the epimerization reaction coordinate. Finally, some of the spectroscopic properties of **5** are at the extremes found for neutral $(\eta^5\text{-}C_5H_5)Re(NO)(PPh_3)(X)$ compounds (e.g., PPh_3 ^{31}P NMR chemical shifts).

The rhenium products of the alkoxide complex cleavage reactions in Schemes II–V can be recycled to ketone complexes by a variety of methods. However, the sequence in Scheme Vb, which converts an optically active alkoxide complex to an optically active ketone complex with only a modest optical activity loss, is clearly optimal. This transformation likely involves the intermediate cationic alcohol complex $[(\eta^5\text{-}C_5H_5)Re(NO)(PPh_3)(HOCH(CH_3)C_6H_5)]^+BF_4^-$ (see Scheme IV). Aldehydes have previously been shown to displace primary alcohols from the corresponding primary alcohol complexes.[29] Ketones would be expected to analogously displace secondary alcohol ligands, although probably at a slower rate.

Although the above methodology has considerable potential for application in asymmetric organic synthesis, there are obvious practical limitations. For example, a stoichiometric quantity of a moderately expensive metal is utilized. However, ketone/nucleophile combinations that would allow rhenium to be employed in catalytic quantities are readily envisioned. Indeed, promising methods for the asymmetric hydride reduction of ketones that employ catalytic amounts of a chiral auxiliary are just beginning to appear.[6c-e]

6. Summary and Conclusions. The chiral Lewis acid $[(\eta^5\text{-}C_5H_5)Re(NO)(PPh_3)]^+$ serves as an effective template for the stereoselective binding and reduction of methyl ketones. The mechanism of asymmetric induction entails (1) formation of a σ complex with the rhenium cis to the smaller methyl substituent and (2) hydride attack upon a rhenium–oxygen conformer in which the bulky PPh_3 ligand blocks one C=O face of the ketone ligand. Stereoselectivities match or exceed those obtained with other chiral hydride reductants.

The alkoxide ligands in the reduction products **5** can be converted to a variety of chiral, optically active organic products. Many of these reactions give optically active rhenium-containing products. Hence, the chiral auxiliary can be recycled without additional optical resolution. Reactions of 3^+X^- with carbon nucleophiles,[5,6] and similar reactions of imine-type complexes,[11] will be described in future publications.

Experimental Section

General Data. All reactions were conducted under a dry inert atmosphere. FT-IR spectra were recorded on Perkin-Elmer 1500 and Mattson Polaris spectrometers. NMR spectra were recorded on Varian XL-300 spectrometers as outlined in Table I unless noted. Optical rotations were measured on a Perkin-Elmer 241 MC polarimeter.[30] UV/visible spectra were recorded on a Perkin-Elmer 552A spectrophotometer. GC analyses were conducted on a Hewlett-Packard 5890 chromatograph (25 m × 0.2 mm SE-54 capillary column). Microanalyses were conducted by Galbraith and Schwarzkopf Laboratories. Melting points were determined in evacuated capillaries.[60]

Acids $HBF_4{\cdot}O(C_2H_5)_2$ (Aldrich) and $HPF_6{\cdot}O(C_2H_5)_2$ (Columbia)[15] were standardized as described previously.[12] Ketones and alcohols were obtained from common commercial sources and fractionally distilled from $CaSO_4$. Borohydride reagents (Aldrich), acetone-*1,3*-$^{13}C_2$ and acetone-*2*-^{13}C (Cambridge Isotope Laboratories; 99% labeled), acetone-d_6 (Stohler), (+)-(*R*)- and (−)-(*S*)-$C_6H_5(CH_3O)(F_3C)CC(=O)OH$ (Aldrich, Fluka), (+)-Eu(hfc)$_3$, (−)-(*S*)-1-phenylethanol, 4-(dimethylamino)pyridine, CF_3CO_2H, and decane (Aldrich) were used as received. $(C_2H_5)_3N$ (Aldrich) was distilled from CaH_2, and (+)-(*S*)-$C_6H_5(CH_3O)(CF_3)CC(=O)Cl$ was prepared as previously described.[34a] Florisil was treated with concentrated NH_4OH (30% v/w).

Solvents were purified as follows: benzene and ether, distilled from Na/benzophenone; pentane, hexane, and toluene, distilled from Na; CH_2Cl_2 and C_6H_5Cl, distilled from P_2O_5; ethyl acetate, used as received; $CDCl_3$, vacuum transferred from P_2O_5; C_6D_6 and CD_2Cl_2, vacuum transferred from CaH_2; $CDFCl_2$ was prepared by a literature procedure.[18]

Preparation of $[(\eta^5\text{-}C_5H_5)Re(NO)(PPh_3)(\eta^1\text{-}O{=}C(CH_3)_2)]^+X^-$ ($3a^+X^-$). **A.** A Schlenk flask was charged with $(\eta^5\text{-}C_5H_5)Re(NO)(PPh_3)(CH_3)$ (**1**,[14] 210 mg, 0.376 mmol), CH_2Cl_2 (15 mL), and a stir bar and was cooled to −80 °C. Next $HBF_4{\cdot}O(C_2H_5)_2$ (0.058 mL, 0.396 mmol) was added with stirring to give $[(\eta^5\text{-}C_5H_5)Re(NO)(PPh_3)(ClCH_2Cl)]^+BF_4^-$ ($2^+BF_4^-$),[12] followed immediately by the addition of acetone (0.083 mL, 1.13 mmol). The solution was allowed to slowly warm to room temperature and was concentrated under oil pump vacuum to 2–3 mL. Ether was added dropwise to precipitate an orange powder, which was collected by filtration and dried under vacuum to give $3a^+BF_4^-$ (204 mg, 0.296 mmol, 79%), mp 178–182 °C dec. UV (nm (ϵ, M^{-1} cm^{-1}), 3.6×10^{-4} M in CH_2Cl_2): 312 sh (2200), 364 sh (1600). Anal. Calcd for $C_{26}H_{26}BF_4NO_2PRe$: C, 45.36; H, 3.81. Found: C, 45.21; H, 3.69. **B.** Complex **1** (142 mg, 0.254 mmol), $HPF_6{\cdot}O(C_2H_5)_2$ (0.019 mL, 0.250 mmol), and acetone (0.073 mL, 1.00 mmol) were combined in a procedure similar to that given for $3a^+BF_4^-$. Workup gave $3a^+PF_6^-$ as a bronze powder, which was extracted with acetone (2–3 mL). Ether was slowly added to the extract by vapor diffusion. Bronze rods of $3a^+PF_6^-$ formed, which were collected by filtration and dried under vacuum (161 mg, 0.216 mmol, 85%), mp 181–184 °C dec. IR (cm^{-1}, KBr) 1685 vs, 1620 m. Anal. Calcd for $C_{26}H_{26}F_6NO_2P_2Re$: C, 41.80; H, 3.51. Found: C, 41.59; H, 3.45. **C.** A Schlenk flask was charged with (+)-(*S*)-**1** (401 mg, 0.718 mmol),[8] acetone (0.160 mL, 2.18 mmol), C_6H_5Cl (2.7 mL), and a stir bar and was cooled to −45 °C. Next $HBF_4{\cdot}O(C_2H_5)_2$ (0.094 mL, 0.752 mmol) was added with stirring. The solution was allowed to slowly warm to room temperature and was then frozen. Ether was layered above the solid, which was slowly thawed. The mixture was gently stirred at room temperature (3–4 h). The resulting orange powder was collected by filtration, washed with ether, and dried under vacuum to give (+)-(*R*)-$3a^+BF_4^-$ (399 mg, 0.579 mmol, 81%), mp 172–176 °C dec, $[\alpha]^{25}_{589}$ 430 ± 4°.[30] IR (cm^{-1}, KBr) 1673 vs, 1616 m. Anal. Found: C, 45.33; H, 3.76. **D.** Complex (+)-(*S*)-**1** (150 mg, 0.268 mmol), CH_2Cl_2 (ca. 25 mL), $HPF_6{\cdot}O(C_2H_5)_2$ (0.059 mL, 0.269 mmol), and acetone (0.100 mL, 1.36 mmol) were combined in a procedure similar to that given for $3a^+PF_6^-$. The solution was slowly warmed to 0 °C and then concentrated under vacuum to ca. 5 mL. Ether was added with stirring. An orange powder precipitated, which was collected by filtration, washed with ether (2 × 10 mL), and dried under vacuum to give (+)-(*R*)-$3a^+PF_6^-$ (133 mg, 0.178 mmol, 66%), mp 175–178 °C dec, $[\alpha]^{25}_{589}$ 528 ± 9°.[30]

Preparation of $[(\eta^5\text{-}C_5H_5)Re(NO)(PPh_3)(\eta^1\text{-}O{=}C(CH_3)CH_2CH_3)]^+X^-$ ($3b^+X^-$). **A.** Complex **1** (286 mg, 0.512 mmol), $HBF_4{\cdot}O(C_2H_5)_2$ (0.078 mL, 0.533 mmol), and 2-butanone (0.137 mL, 1.53 mmol) were combined in a procedure similar to that given for $3a^+BF_4^-$. Workup gave $3b^+BF_4^-$ as an orange powder (311 mg, 0.443 mmol, 86%), mp 145–149 °C dec. Anal. Calcd for $C_{27}H_{28}BF_4NO_2PRe$: C, 46.16; H, 4.02. Found: C, 46.09; H, 4.13. **B.** Complex **1** (397 mg, 0.702 mmol), $HPF_6{\cdot}O(C_2H_5)_2$ (0.521 mL, 0.702 mmol), and 2-butanone (0.313 mL, 3.50 mmol) were combined in a procedure similar to that given for $3a^+PF_6^-$. Workup gave $3b^+PF_6^-$ as a light orange powder, which was extracted with CH_2Cl_2 (3–5 mL). Ether was slowly added to the extract by vapor diffusion. This gave orange-red rods of $3b^+PF_6^-$, which were collected by filtration and dried under vacuum (471 mg, 0.624 mmol, 89%), mp 148–150 °C dec. IR (cm^{-1}, KBr) 1690 vs, 1623 m. Anal. Calcd for $C_{27}H_{28}F_6NO_2P_2Re$: C, 41.28; H, 3.63. Found: C, 41.22; H, 3.91. **C.** Complex (+)-(*S*)-**1** (206 mg, 0.369 mmol), $HBF_4{\cdot}O(C_2H_5)_2$ (0.053 mL, 0.389 mmol), and 2-butanone (0.231 mL, 2.58 mmol) were combined in a procedure similar to that given for $3b^+BF_4^-$. The solution was filtered through Celite when it reached room temperature. The filtrate was concentrated under vacuum to ca. 1 mL, and ether was added. An orange powder precipitated, which was collected by filtration and dried under vacuum to give (+)-(*R*)-$3b^+BF_4^-$ (201 mg, 0.286 mmol, 78%), mp 154–158 °C dec, $[\alpha]^{25}_{589}$ 490 ± 5°.[30] IR (cm^{-1}, KBr) 1675 vs, 1617 m. Anal. Found: C, 46.27; H, 4.30. **D.** Complex (+)-(*S*)-**1** (300 mg, 0.537 mmol), $HPF_6{\cdot}O(C_2H_5)_2$ (0.098 mL, 0.539 mmol), and 2-butanone (0.240 mL, 2.68 mmol) were combined in a procedure similar to that given for (+)-(*R*)-$3a^+PF_6^-$. An identical workup gave (+)-(*R*)-$3b^+PF_6^-$ as an orange powder (261 mg, 0.343 mmol, 64%), mp 137–140 °C dec, $[\alpha]^{25}_{589}$ 422 ± 8°.[30]

Preparation of $[(\eta^5\text{-}C_5H_5)Re(NO)(PPh_3)(\eta^1\text{-}O{=}C(CH_3)CH(CH_3)_2)]^+BF_4^-$ ($3c^+BF_4^-$). **A.** Complex **1** (204 mg, 0.366 mmol), $HBF_4{\cdot}O(C_2H_5)_2$ (0.056 mL, 0.383 mmol), and 3-methyl-2-butanone (0.117 mL, 1.09 mmol) were combined in a procedure similar to that given for $3a^+BF_4^-$. Workup gave $3c^+BF_4^-$ as an orange powder (219 mg, 0.306 mmol, 84%), mp 159–161 °C dec. Anal. Calcd for $C_{28}H_{30}BF_4NO_2PRe$: C, 46.93; H, 4.22. Found: C, 46.99; H, 4.33. **B.** Complex (+)-(*S*)-**1** (219 mg, 0.392 mmol), $HBF_4{\cdot}O(C_2H_5)_2$ (0.056 mL,

(60) Tiers, G. V. D. *J. Chem. Educ.* **1990**, *67*, 258.
(61) Buhro, W. E.; Zwick, B. D.; Georgiou, S.; Hutchinson, J. P.; Gladysz, J. A. *J. Am. Chem. Soc.* **1988**, *110*, 2427.

0.448 mmol), and 3-methyl-2-butanone (0.294 mL, 2.74 mmol) were combined in a procedure similar to that given for (+)-(*R*)-**3b**$^+BF_4^-$. Workup gave (+)-(*R*)-**3c** as an orange powder (219 mg, 0.306 mmol, 78%), mp 143–148 °C dec, $[\alpha]^{25}_{589}$ 410 ± 4°.[30] IR (cm^{-1}, KBr) 1694 vs, 1612 m. Anal. Found: C, 47.09; H, 4.31.

Preparation of [(η^5-C_5H_5)Re(NO)(PPh$_3$)(η^1-O=C(CH$_3$)C(CH$_3$)$_3$)]$^+$ BF_4^- (**3d**$^+BF_4^-$). **A.** Complex **1** (485 mg, 0.868 mmol), $HBF_4{\cdot}O(C_2H_5)_2$ (0.133 mL, 0.912 mmol), and 3,3-dimethyl-2-butanone (0.326 mL, 2.61 mmol) were combined in a procedure similar to that given for **3a**$^+BF_4^-$. Workup gave **3d**$^+BF_4^-$ as an orange powder (540 mg, 0.739 mmol, 85%), mp 149–154 °C dec. Anal. Calcd for $C_{29}H_{32}BF_4NO_2PRe$: C, 47.68; H, 4.41. Found: C, 47.69; H, 4.47. **B.** Complex (+)-(*S*)-**1** (421 mg, 0.754 mmol), $HBF_4{\cdot}O(C_2H_5)_2$ (0.100 mL, 0.800 mmol), and 3,3-dimethyl-2-butanone (0.250 mL, 2.00 mmol) were combined in a procedure similar to that given for (+)-(*R*)-**3a**$^+BF_4^-$. Workup gave (+)-(*R*)-**3d**$^+$ BF_4^- as an orange powder (455 mg, 0.623 mmol, 83%), mp 171–174 °C dec, $[\alpha]^{25}_{589}$ 380 ± 4°.[30] IR (cm^{-1}, KBr) 1686 vs, 1606 m. Anal. Found: C, 47.60; H, 4.50.

Preparation of [(η^5-C_5H_5)Re(NO)(PPh$_3$)(η^1-O=C(CH$_3$)C$_6$H$_5$)]$^+$X$^-$ (**3e**$^+$X$^-$). **A.** Complex **1** (286 mg, 0.512 mmol), $HBF_4{\cdot}O(C_2H_5)_2$ (0.078 mL, 0.533 mmol), and acetophenone (0.179 mL, 1.53 mmol) were combined in a procedure similar to that given for **3a**$^+BF_4^-$. Workup gave **3e**$^+BF_4^-$ as a red powder (328 mg, 0.437 mmol, 85%), mp 167–170 °C dec. UV/visible (nm (ϵ, M^{-1} cm^{-1}), 3.5 × 10^{-4} M in CH_2Cl_2): 260 sh (18700), 433 pk (5300). Anal. Calcd for $C_{31}H_{28}BF_4NO_2PRe$: C, 49.61; H, 3.76. Found: C, 49.28; H, 3.79. **B.** Complex **1** (204 mg, 0.363 mmol), $HPF_6{\cdot}O(C_2H_5)_2$ (0.028 mL, 0.362 mmol), and acetophenone (0.168 mL, 1.44 mmol) were combined in a procedure similar to that given for **3b**$^+PF_6^-$. An identical crystallization gave red rods of **3e**$^+PF_6^-$ (254 mg, 0.312 mmol, 86%), mp 175–179 °C dec. IR (cm^{-1}, KBr) 1684 vs, 1558 m. Anal. Calcd for $C_{31}H_{28}F_6NO_2P_2Re$: C, 46.04; H, 3.46. Found: C, 45.90; H, 3.50. **C.** Complex (+)-(*S*)-**1** (216 mg, 0.387 mmol), $HBF_4{\cdot}O(C_2H_5)_2$ (0.051 mL, 0.408 mmol), and acetophenone (0.090 mL, 0.771 mmol) were combined in a procedure similar to that given for (+)-(*R*)-**3a**$^+BF_4^-$. Workup gave (+)-(*R*)-**3e**$^+BF_4^-$ as a red powder (272 mg, 0.362 mmol, 94%), mp 103–106 °C dec, $[\alpha]^{25}_{589}$ 770 ± 8°.[30] IR (cm^{-1}, KBr) 1686 vs, 1559 m. Anal. Found: C, 49.51; H, 3.75. **D.** Complex (+)-(*S*)-**1** (239 mg, 0.428 mmol), $HPF_6{\cdot}O(C_2H_5)_2$ (0.078 mL, 0.429 mmol), and acetophenone (0.250 mL, 2.14 mmol) were combined in a procedure similar to that given for (+)-(*R*)-**3a**$^+PF_6^-$. An identical workup gave (+)-(*R*)-**3e**$^+PF_6^-$ as a red powder (195 mg, 0.241 mmol, 56%), mp 112–116 °C dec, $[\alpha]^{25}_{589}$ 860 ± 18°.[30]

Preparation of (η^5-C_5H_5)Re(NO)(PPh$_3$)(OCH(CH$_3$)$_2$) (**5a**). **A.** A Schlenk flask was charged with **3a**$^+BF_4^-$ (87 mg, 0.126 mmol), CH_2Cl_2 (15 mL), and a stir bar and was cooled to −80 °C. Next K(*sec*-C_4H_9)$_3$BH (0.129 mL, 1 M in THF) was added with stirring, and the solution was allowed to slowly warm to room temperature. The solvent was removed under vacuum, and the residue was extracted with benzene. The extracts were filtered through a 2 × 2 cm column of CaO, and the solvent was removed under vacuum. This gave **5a** as an orange solid (66 mg, 0.110 mmol, 87%), mp 175–180 °C dec. Anal. Calcd for $C_{26}H_{27}NO_2PRe$: C, 51.82; H, 4.52. Found: C, 51.77; H, 4.39. **B.** Complex (+)-(*R*)-**3a**$^+BF_4^-$ (99 mg, 0.144 mmol), CH_2Cl_2 (2 mL), and K(*sec*-C_4H_9)$_3$BH (0.150 mL, 1 M in THF) were combined in a procedure identical with that given for **3a**$^+BF_4^-$. The extracts were filtered through a 1 × 6 cm column of CaO, and the solvent was removed under vacuum. The residue was dissolved in ether, and hexane was added. The solution was concentrated under vacuum. An orange powder precipitated, which was dried under vacuum to give (+)-(*R*)-**5a** (47 mg, 0.078 mmol, 54%), mp 186–188 °C dec, $[\alpha]^{25}_{589}$ 390 ± 8°.[30] Anal. Found: C, 51.55; H, 4.65.

Preparation of (η^5-C_5H_5)Re(NO)(PPh$_3$)(OCH(CH$_3$)CH$_2$CH$_3$) (**5b**). **A.** Complex **3b**$^+BF_4^-$ (129 mg, 0.184 mmol) and K(*sec*-C_4H_9)$_3$BH (0.190 mL, 1 M in THF) were combined in a procedure similar to that given for **5a**. Workup gave (*RS*,*SR*)-**5b** as an orange solid (103 mg, 0.167 mmol, 91%; de:[28] Scheme II), mp 169–172 °C dec. Anal. Calcd for $C_{27}H_{29}NO_2PRe$: C, 52.58; H, 4.74. Found: C, 52.71; H, 4.87. **B.** Complex (+)-(*R*)-**3b**$^+BF_4^-$ (100 mg, 0.143 mmol) and K(*sec*-C_4H_9)$_3$BH (0.150 mL, 1 M in THF) were combined in a procedure similar to that given for (+)-(*R*)-**5a**. Workup gave (+)-(*RS*)-**5b** as an orange solid (78 mg, 0.127 mmol, 89%; de: Scheme II), mp 150–154 °C dec, $[\alpha]^{25}_{589}$ 510 ± 5°.[30] Anal. Found: C, 52.91; H, 4.94. **C.** A Schlenk tube was charged with **3b**$^+BF_4^-$ (27.3 mg, 0.039 mmol), CH_2Cl_2 (1 mL), and a stir bar and was cooled to −80 °C. A solution of (η^5-C_5H_5)Re(NO)-(PPh$_3$)(CHO) (**7**;[10c,14] 25.0 mg, 0.044 mmol) in CH_2Cl_2 (0.5 mL) was slowly added down the wall of the tube by cannula. The cannula was then rinsed with CH_2Cl_2 (1 mL). The solution was stirred at −80 °C for 3 h and then allowed to slowly warm to room temperature. The solvent was removed under vacuum, and the residue was extracted with benzene. The extracts were filtered through a 2 × 2 cm column of CaO, and the solvent was removed under vacuum. This gave (*RS*,*SR*)-**5b** as an orange solid (21.0 mg, 0.034 mmol, 87%; de: Scheme III). **D.** Complex (+)-(*R*)-**3b**$^+BF_4^-$ (11.1 mg, 0.016 mmol) and **7** (9.8 mg, 0.017 mmol) were combined in a procedure identical with procedure **C**. Workup gave (+)-(*RS*)-**5b** as an orange solid (5.3 mg, 0.009 mmol, 56%; de: Scheme III). **E.** Complex (+)-(*R*)-**3b**$^+BF_4^-$ (29.9 mg, 0.043 mmol) and (+)-(*S*)-**7**-d_1[10c] (24.4 mg, 0.043 mmol) were combined in a procedure identical with procedure **C**. The mixture was kept at −80 °C for 16 h. Workup employed a base-treated Florisil column[10c] and gave (+)-(*RS*)-**5b**-d_1 as an orange solid (24.5 mg, 0.040 mmol, 93%; de: Scheme III). **F.** Complex (+)-(*R*)-**3b**$^+BF_4^-$ (30.0 mg, 0.043 mmol) and (−)-(*R*)-**7**-d_1[10c] (25.1 mg, 0.044 mmol) were combined in a procedure identical with procedure **E**. Workup gave (+)-(*RS*)-**5b**-d_1 as an orange solid (20.1 mg, 0.033 mmol, 78%; de: Scheme III). **G.** A Schlenk flask was charged with **1** (109 mg, 0.195 mmol), CH_2Cl_2 (1 mL), and a stir bar and was cooled to −80 °C. Next $HBF_4{\cdot}O(C_2H_5)_2$ (0.029 mL, 0.232 mmol) and 2-butanol (0.350 mL, 3.81 mmol) were sequentially added with stirring. After 5 min, the flask was transferred to a 0 °C bath. After 15 min, solvent was removed under vacuum. The residue was cooled to −80 °C, and CH_2Cl_2 (3 mL) and $(C_2H_5)_3N$ (0.500 mL, 3.59 mmol) were sequentially added with stirring. After 5 min, the flask was removed from the low-temperature bath. After 15 min, solvent was removed under vacuum. The residue was extracted with benzene, and the extracts were filtered through base-treated Florisil. Solvent was removed from the filtrate under vacuum. The residue was dissolved in ether and hexane was added. The solvents were removed by vacuum with rapid stirring. This gave **5b** as an orange powder ((53 ± 2):(47 ± 2) (*RS*,*SR*)/(*RR*,*SS*)), which was dried under vacuum (111 mg, 0.180 mmol, 92%), mp 169–173 °C dec. Anal. Found: C, 52.41; H, 4.70. **H.** NMR data on (*RR*,*SS*)-**5b**: ^{1}H (δ, C_6D_6) 7.75–6.99 (m, 3 C_6H_5), 4.85 (s, C_5H_5), 3.41 (m, OCH), 2.07 (d, J_{HH} = 6.0 Hz, OCCH_3), 1.06 (m, CH_2), 1.00 (t, J_{HH} = 7.5 Hz, CH_2CH_3); ^{13}C{^{1}H} (ppm, C_6D_6) PPh$_3$ at 135.7 (d, J_{CP} = 50.5 Hz, *i*), 134.6 (d, J_{CP} = 10.4 Hz), 130.2 (d, J_{CP} = 2.0 Hz, *p*); 90.8 (d, J_{CP} = 2.1 Hz, C_5H_5), 90.2 (d, J_{CP} = 6.1 Hz, OC), 33.3 (s, CH_2), 23.8 (s, OCCH_3), 10.8 (s, CH_2CH_3); ^{31}P{^{1}H} (ppm, C_6D_6) 16.4 (s).

Preparation of (η^5-C_5H_5)Re(NO)(PPh$_3$)(OCH(CH$_3$)CH(CH$_3$)$_2$) (**5c**). **A.** Complex **3c**$^+BF_4^-$ (109 mg, 0.152 mmol) and K(*sec*-C_4H_9)$_3$BH (0.155 mL, 1 M in THF) were combined in a procedure similar to that given for **5a**. Workup gave (*RS*,*SR*)-**5c** as an orange solid (88 mg, 0.140 mmol, 92%; de:[28] Scheme II), mp 134–136 °C dec. Anal. Calcd for $C_{28}H_{31}NO_2PRe$: C, 53.32; H, 4.95. Found: C, 53.60; H, 4.93. **B.** Complex (+)-(*R*)-**3c**$^+BF_4^-$ (105 mg, 0.147 mmol) and K(*sec*-C_4H_9)$_3$BH (0.154 mL, 1 M in THF) were combined in a procedure similar to that given for (+)-(*R*)-**5a**. Workup gave (+)-(*RS*)-**5c** as an orange solid (83 mg, 0.132 mmol, 90%; de: Scheme II), mp 112–114 °C dec, $[\alpha]^{25}_{589}$ 520 ± 5°.[30] Anal. Found: C, 53.16; H, 4.83. **C.** Complex **1** (100 mg, 0.179 mmol), $HBF_4{\cdot}O(C_2H_5)_2$ (0.024 mL, 0.192 mmol), 3-methyl-2-butanol (0.380 mL, 3.53 mmol), and $(C_2H_5)_3N$ (0.500 mL, 3.59 mmol) were reacted in a procedure similar to procedure **G** for **5b**. Workup gave **5c** as an orange powder (98 mg, 0.155 mmol, 87%; (77 ± 2):(23 ± 2) (*RS*,*SR*)/(*RR*,*SS*)), mp 164–170 °C dec. **D.** NMR data on (*RR*,*SS*)-**5c**: ^{1}H (δ, C_6D_6) 7.80–6.90 (m, 3 C_6H_5), 4.85 (s, C_5H_5), 3.48 (m, OCH), 2.16 (m, CH(CH$_3$)$_2$), 1.49 (d, J_{HH} = 5.9 Hz, OCCH_3), 1.00 (d, J_{HH} = 7.0 Hz, CHCH_3), 0.94 (d, J_{HH} = 6.2 Hz, CHCH'_3); ^{13}C{^{1}H} (ppm, C_6D_6) PPh$_3$ at 135.5 (d, J_{CP} = 50.4 Hz, *i*), 134.4 (d, J_{CP} = 10.2 Hz), 130.1 (s, *p*); 93.8 (d, J_{CP} = 6.0 Hz, OC), 90.7 (s, C_5H_5), 35.1 (s), 20.1 (s), 18.7 (s), 16.5 (s); ^{31}P{^{1}H} (ppm, C_6D_6) 15.9 (s).

Preparation of (η^5-C_5H_5)Re(NO)(PPh$_3$)(OCH(CH$_3$)C(CH$_3$)$_3$) (**5d**). **A.** Complex **3d**$^+BF_4^-$ (124 mg, 0.170 mmol) and K(*sec*-C_4H_9)$_3$BH (0.178 mL, 1 M in THF) were combined in a procedure similar to that given for **5a**. Workup gave (*RS*,*SR*)-**5d** as an orange solid (84 mg, 0.131 mmol, 77%; de:[28] Scheme II), mp 149–156 °C dec. Anal. Calcd for $C_{29}H_{33}NO_2PRe$: C, 54.02; H, 5.16. Found: C, 54.19; H, 5.57. **B.** Complex (+)-(*R*)-**3d**$^+BF_4^-$ (68 mg, 0.094 mmol) and K(*sec*-C_4H_9)$_3$BH (0.098 mL, 1 M in THF) were combined in a procedure similar to that given for (+)-(*R*)-**5a**. Workup gave (+)-(*RS*)-**5d** as an orange solid (47 mg, 0.073 mmol, 78%; de: Scheme II), mp 191–194 °C dec, $[\alpha]^{25}_{589}$ 455 ± 5°.[30] Anal. Found: C, 53.85; H, 5.16. **C.** Complex (−)-(*S*)-**3d**$^+BF_4^-$ (112 mg, 0.153 mmol) and K(*sec*-C_4H_9)$_3$BH (0.164 mL, 1 M in THF) were combined in a procedure similar to that given for (+)-(*R*)-**5a**. Workup gave (−)-(*SR*)-**5d** as an orange solid (72 mg, 0.112 mmol, 73%; de: Scheme II). **D.** Complex **1** (108 mg, 0.193 mmol), $HBF_4{\cdot}O(C_2H_5)_2$ (0.029 mL, 0.232 mmol), 3,3-dimethyl-2-butanol (0.500 mL, 3.97 mmol), and $(C_2H_5)_3N$ (0.500 mL, 3.59 mmol) were reacted in a procedure similar to procedure **G** for **5b**. Workup gave **5d** as an orange powder (94 mg, 0.146 mmol, 76%; (61 ± 2):(39 ± 2) (*RS*,*SR*)/(*RR*,*SS*)), mp 195–199 °C dec. Anal. Found: C, 54.29; H, 5.28. **E.** NMR data on (*RR*,*SS*)-**5d**: ^{1}H (δ, C_6D_6) 7.70–7.00 (m, 3 C_6H_5), 4.87 (s, C_5H_5), 3.46 (q, J_{HH} = 6.1 Hz, OCH), 0.99 (s, C(CH$_3$)$_3$), 0.95 (d, J_{HH} = 6.2 Hz,

$OCCH_3$): $^{13}C\{^1H\}$ (ppm, C_6D_6) PPh_3 at 136.1 (d, J_{CP} = 50.1 Hz, *i*), 134.6 (d, J_{CP} = 10.5 Hz), 130.2 (s, *p*); 98.3 (d, J_{CP} = 6.1 Hz, OC), 90.8 (s, C_5H_5), 37.1 (s, $C(CH_3)_3$), 27.2 (s, $C(CH_3)_3$), 19.2 (s, $OCCH_3$); $^{31}P\{^1H\}$ (ppm, C_6D_6) 17.1 (s).

Preparation of $(\eta^5\text{-}C_5H_5)Re(NO)(PPh_3)(OCH(CH_3)C_6H_5)$ (5e). **A.** Complex **3e**$^+BF_4^-$ (134 mg, 0.178 mmol) and K(*sec*-$C_4H_9)_3BH$ (0.182 mL, 1 M in THF) were combined in a procedure similar to that given for **5a**. Workup gave (*RS,SR*)-**5e** as an orange solid (107 mg, 0.161 mmol, 90%; de:[28] Scheme II), mp 162–163 °C dec. Anal. Calcd for $C_{31}H_{29}NO_2PRe$: C, 56.01; H, 4.40. Found: C, 55.82; H, 4.42. **B.** Complex (+)-(*R*)-**3e**$^+BF_4^-$ (105 mg, 0.140 mmol) and K(*sec*-$C_4H_9)_3BH$ (0.150 mL, 1 M in THF) were combined in a procedure similar to that given for (+)-(*R*)-**5a**. Workup gave (+)-(*RS*)-**5e** as an orange solid (85 mg, 0.129 mmol, 92%; de: Scheme II), mp 124–128 °C dec, $[\alpha]^{25}_{589}$ 418 ± 5°.[30] Anal. Found: C, 56.04; H, 4.71. **C.** Complex **3e**$^+BF_4^-$ (25.6 mg, 0.034 mmol) and **7** (21.4 mg, 0.037 mmol) were combined in a procedure similar to procedure **C** for **5b**. Workup gave (*RS,SR*)-**5e** as an orange solid (20.8 mg, 0.031 mmol, 91%; de: Scheme III). **D.** Complex (+)-(*R*)-**3e**$^+BF_4^-$ (10.4 mg, 0.014 mmol) and **7** (8.4 mg, 0.015 mmol) were combined in a procedure similar to procedure **D** for **5b**. Workup gave (+)-(*RS*)-**5e** as an orange solid (5.6 mg, 0.009 mmol, 64%; de: Scheme III). **E.** Complex **1** (121 mg, 0.217 mmol), $HBF_4{\cdot}O(C_2H_5)_2$ (0.029 mL, 0.232 mmol), 1-phenylethanol (0.130 mL, 0.217 mmol), and $(C_2H_5)_3N$ (0.500 mL, 3.59 mmol) were reacted in a procedure similar to procedure **G** for **5b**. Workup gave **5e** as an orange powder that contained unvolatilized alcohol (136 mg, 0.204 mmol, 95%; (82 ± 2):(18 ± 2) (*RS,SR*)/(*RR,SS*)). **F.** NMR data on (*RR,SS*)-**5d**: ^1H (δ, C_6D_6) 7.76–7.02 (m, 4 C_6H_5), 4.82 (s, C_5H_5), 4.56 (q, J_{HH} = 6.3 Hz, OCH), 1.38 (d, J_{HH} = 6.3 Hz, CH_3); $^{13}C\{^1H\}$ (ppm, C_6D_6, partial) PPh_3 at 135.5 (d, J_{CP} = 10.4 Hz), 130.1 (d, J_{CP} = 2.1 Hz, *p*); 91.6 (d, J_{CP} = 6.2 Hz, OC), 90.6 (s, C_5H_5), 27.7 (s, CH_3); $^{31}P\{^1H\}$ (ppm, C_6D_6) 16.3 (s).

Preparation of $(\eta^5\text{-}C_5H_5)Re(NO)(PPh_3)(OC(=O)C(CF_3)(OCH_3)C_6H_5)$ (11). **A.** A Schlenk flask was charged with (+)-(*S*)-**1** (80 mg, 0.143 mmol), (+)-(*R*)-$C_6H_5(CH_3O)(F_3C)CC(=O)OH$ ((+)-(*R*)-MTPA; 166 mg, 0.709 mmol), benzene (2 mL), and a stir bar. The solution was stirred for 48 h and then filtered through CaO. Solvent was removed from the filtrate under vacuum. The resulting oil was chromatographed on silica (50:50 ethyl acetate–hexane). Solvent was removed from the red band. The resulting oil was dissolved in benzene (2 mL). Pentane was added by vapor diffusion. Orange plates formed, which were collected by filtration and dried under vacuum to give (+)-(*RR*)-**11** (76 mg, 0.098 mmol, 68%; 99% de by ^1H NMR), mp 153–155 °C dec, $[\alpha]^{25}_{589}$ 390 ± 4°.[30] Anal. Calcd for $C_{33}H_{28}F_3NO_4PRe$: C, 51.03; H, 3.63. Found: C, 51.04; H, 3.66. IR (cm^{-1}, KBr): 1676 (vs, ν_{CO}), 1648 (vs, ν_{NO}). ^1H NMR (δ, $CDCl_3$) 7.53–7.26 (m, 4 C_6H_5), 5.28 (s, C_5H_5), 3.07 (q, J_{HF} = 1.0 Hz, CH_3). $^{13}C\{^1H\}$ NMR (ppm, $CDCl_3$) 172.7 (s, CO), PPh_3 at 133.7 (d, J_{CP} = 53.3 Hz, *i*), 133.4 (d, J_{CP} = 10.8 Hz), 130.4 (s, *p*), 128.4 (d, J_{CP} = 10.0 Hz); CPh at 133.7 (s, *i*), 128.3 (s, *p*), 127.7 (s), 127.6 (s); 123.6 (q, J_{CF} = 287.4 Hz, CF_3), 90.8 (s, C_5H_5), 83.4 (q, J_{CF} = 25.8 Hz, CPh), 54.4 (s, CH_3). $^{31}P\{^1H\}$ NMR (ppm, $CDCl_3$) 19.7 (s). **B.** Complex (+)-(*S*)-**1** (58 mg, 0.104 mmol), (−)-(*S*)-MTPA (124 mg, 0.529 mmol), and benzene (2 mL) were combined in a procedure similar to that given for (+)-(*RR*)-**11**. Workup gave (+)-(*RS*)-**11** as red hexagonal crystals (62 mg, 0.080 mmol, 77%; >99% de by ^1H NMR), mp 148–151 °C dec, $[\alpha]^{25}_{589}$ 410 ± 4°.[30] Anal. Found: C, 51.05; H, 3.61. IR (cm^{-1}, KBr): 1687 (vs, ν_{CO}), 1648 (vs, ν_{NO}). ^1H NMR (δ, $CDCl_3$) 7.41–7.16 (m, 4 C_6H_5), 5.20 (s, C_5H_5), 3.18 (q, J_{HF} = 1.0 Hz, CH_3). $^{13}C\{^1H\}$ NMR (ppm, $CDCl_3$) 173.2 (s, CO), PPh_3 at 133.6 (d, J_{CP} = 53.1 Hz, *i*), 133.4 (d, J_{CP} = 10.8 Hz), 130.4 (s, *p*), 128.4 (d, J_{CP} = 10.2 Hz); CPh at 134.2 (s, *i*), 128.1 (s, *p*), 127.6 (s), 126.8 (s); 123.9 (q, J_{CF} = 287.7 Hz, CF_3), 90.8 (s, C_5H_5), 83.0 (q, J_{CF} = 25.1 Hz, CPh), 54.8 (s, CH_3). $^{31}P\{^1H\}$ NMR (ppm, $CDCl_3$), 19.2 (s). **C.** A 5-mm NMR tube was charged with (+)-(*RS*)-**5c** (19 mg, 0.030 mmol), (−)-(*S*)-MTPA (8 mg, 0.034 mmol), and C_6D_6 (0.700 mL) and capped with a septum. A ^1H NMR spectrum showed complete conversion to (+)-(*RS*)-**11** (<5 min, ≥99% de). The solution was filtered through CaO, and solvent was removed under vacuum to give (+)-(*RS*)-**11** (22 mg, 0.028 mmol, 93%). **D.** Complex (+)-(*RS*)-**5d** (16 mg, 0.025 mmol) and (−)-(*S*)-MTPA (10 mg, 0.043 mmol) were combined in a procedure similar to procedure **C**. Workup gave (+)-(*RS*)-**11** (18 mg, 0.023 mmol, 92%; >99% de).

Preparation of $C_6H_5(CH_3O)(F_3C)CC(=O)OCH(CH_3)R$ (10). **A.** A Schlenk flask was charged with (+)-(*RS*)-**5b** (43 mg, 0.070 mmol), 4-(dimethylamino)pyridine (DMAP; 12 mg, 0.099 mmol), (+)-(*S*)-$C_6H_5(CH_3O)(F_3C)CC(=O)Cl$ (MTPACl; 0.020 mmol, 0.106 mmol), benzene (3 mL), and a stir bar. The mixture was stirred at 50 °C for 2 h, cooled, and passed through a glass microfiber filter. Solvent was removed by rotary evaporation in the presence of silica. The silica was flash chromatographed with hexane (100 mL) and then ethyl acetate–hexane (2:98, v/v). Solvent was removed from the ethyl acetate–hexane fractions to give previously characterized[34] (*RS*)-**10b** (20 mg, 0.069 mmol, 99%; de: Scheme II) as a clear colorless oil. **B.** Complex (+)-(*RS*)-**5c** (43 mg, 0.068 mmol), DMAP (11 mg, 0.090 mmol), (+)-(*S*)-MTPACl (0.019 mmol, 0.101 mmol), and benzene (3 mL) were combined in a procedure similar to procedure **A**. An identical workup gave previously characterized[34] (*RS*)-**10c** (20 mg, 0.066 mmol, 97%; de: Scheme II) as a clear colorless oil. **C.** Complex (+)-(*RS*)-**5d** (38 mg, 0.059 mmol), DMAP (9 mg, 0.074 mmol), (+)-(*S*)-MTPACl (0.020 mL, 0.107 mmol), and benzene (4 mL) were combined in a procedure similar to procedure **A** but were first stirred at room temperature for 36 h. The mixture was then stirred at 50 °C for 6 h. An identical workup gave previously characterized[34] (*RS*)-**10d** (18 mg, 0.056 mmol, 95%; de: Scheme II) as a clear colorless oil. **D.** Complex (+)-(*RS*)-**5e** (45 mg, 0.068 mmol), DMAP (12 mg, 0.098 mmol), (+)-(*S*)-MTPACl (0.024 mL, 0.128 mmol), and benzene (4 mL) were combined in a procedure similar to procedure **C**. An identical reaction period and workup gave (*RS*)-**10e** (22 mg, 0.065 mmol, 96%; de: Scheme II)[34] as a clear colorless oil.

Reaction of (+)-(*RS*)-5e, $HBF_4{\cdot}O(C_2H_5)_2$, and 2-Butanone. A Schlenk flask was charged with (+)-(*RS*)-**5e** (57 mg, 0.086 mmol), CH_2Cl_2 (3 mL), and a stir bar and was cooled to −80 °C. Next $HBF_4{\cdot}O(C_2H_5)_2$ (0.011 mL, 0.088 mmol) and 2-butanone (0.150 mL, 1.67 mmol) were sequentially added with stirring. The solution was allowed to slowly warm to room temperature, kept at room temperature for 2 h, and then cooled to 0 °C for 6 h. Ether (6 mL) was added, and an orange powder precipitated. Decane (0.002 mL) was then added, and GC analysis showed a 71 ± 2% yield of 1-phenylethanol. The orange powder was collected by filtration, washed with ether, and dried under vacuum to give (+)-(*R*)-**3b**$^+BF_4^-$ (47 mg, 0.067 mmol, 78%), $[\alpha]^{25}_{589}$ 454 ± 4° (93 ± 1% ee).[30]

Labeling, Rate, and Dynamic NMR Experiments. **A.** Deuterium and ^{13}C-labeled derivatives of **3a**$^+BF_4^-$ were prepared from **2**$^+BF_4^-$ and the appropriately labeled acetone. IR (cm^{-1}, KBr) **3a**$^+$-$^{13}C_2BF_4^-$ 1679 s, 1624 s; **3a**$^+$-$^{13}CBF_4^-$ 1679 vs, 1582 m. **B.** A 5-mm NMR tube was charged with **3a**$^+BF_4^-$ (31 mg, 0.045 mmol) and CD_2Cl_2 (0.700 mL) and capped with a septum. A ^1H NMR spectrum was recorded. Next acetone-d_6 (0.055 mL, 0.748 mmol) was added, and ligand exchange was monitored by disappearance of the **3a**$^+BF_4^-$ methyl resonance (13 h, 28 °C). Data were treated by standard pseudo-first-order methods[17] as detailed elsewhere.[35] **C.** Variable-temperature NMR experiments were conducted as described previously.[61] Probe temperatures were calibrated with either methanol (low temperatures) or ethylene glycol (high temperatures) and were assumed to be accurate to ±1 °C. Rate constants and ΔG^* were calculated by standard methods.[19]

Crystal Structure of 3e$^+PF_6^-$. A dark red rod, grown as described above, was mounted on a glass fiber. Axial photographs showed monoclinic symmetry. Unit cell dimensions were obtained by least-squares refinement with use of 25 centered reflections for which 25° < 2θ < 37°. Data were collected on a Nicolet R3m/E four-circle diffractometer as outlined in Table II.

Data reduction[62] included corrections for Lorentz and polarization effects. Non-hydrogen atoms were refined with anisotropic thermal parameters by blocked cascade least squares, minimizing $\sum W\Delta^2$, with 101 parameters refined in each full-matrix block. Scattering factors were taken from the literature.[63] Absorption corrections were calculated by Gaussian integration with use of measured distances between indexed crystal faces. Calculated hydrogen positions were used during refinement, with a common refined isotropic thermal parameter for phenyl and cyclopentadienyl hydrogens. The methyl hydrogens were given thermal parameters 1.2 times the equivalent isotropic thermal parameter of the methyl carbon. No corrections were made for extinction.

Crystal Structure of 3a$^+PF_6^-$. A bronze rod, grown as described above, was mounted on a glass fiber. The unit cell determination, data collection, and data reduction were conducted as for **3e**$^+PF_6^-$. Empirical absorption corrections were based on the azimuthal scan data. Hydrogen atoms were refined as above. Four reflections showing strong extinction effects were excluded from the final refinement.

Crystal Structure of (*RS,SR*)-5e. A red crystal (grown from layered toluene–hexane) was mounted on a glass fiber for preliminary data collection on a Syntex $P\bar{1}$ diffractometer. Lattice parameters (Table II) were determined from 15 centered reflections with 21° < 2θ < 24°. The space group was determined from systematic absences ($h0l$ l = 2n, $0k0$ k = 2n). Lorentz and polarization corrections, and an empirical ab-

(62) Crystallographic calculations were performed on a Data General Eclipse computer with the SHELXTL program package by G. M. Sheldrick, Nicolet Analytical Instruments, Madison, WI, 1983.

(63) Cromer, D. T.; Waber, J. T. In *International Tables for X-ray Crystallography*; Ibers, J. A., Hamilton, W. C., Eds.; Kynoch: Birmingham, England, 1974; Vol. IV, pp 72–98, 149–150; Tables 2.2B and 2.3.1.

sorption correction based upon a series of ψ scans, were applied. Intensities of equivalent reflections were averaged, and 12 reflections were rejected because their intensities differed significantly from the average. The structure was solved by standard heavy-atom techniques with the SDP/VAX package.[64] All non-hydrogens were refined with anisotropic thermal parameters. Hydrogen positions were calculated except for H1, which was located from a difference map. Additional details are given elsewhere.[35]

Acknowledgment. We thank the NIH for support of this research, Mr. N. Quirós Méndez for UV/visible spectra, and Dr. C. M. Garner for assistance with entries 5 and 6 of Scheme III.

Supplementary Material Available: Tables of atomic coordinates and anisotropic thermal parameters for **3a**,$e^+PF_6^-$ and (*RS*,*SR*)-**5e** (6 pages); tables of calculated and observed structure factors for **3a**,$e^+PF_6^-$ and (*RS*,*SR*)-**5e** (71 pages). Ordering information is given on any current masthead page.

(64) The Enraf-Nonius CAD 4 SDP—A Real-time System for Concurrent X-ray Data Collection and Crystal Structure Determination. Frenz, B. A. In *Computing and Crystallography*; Schenk, H., Olthof-Hazelkamp, R., van Konigsveld, H., Bassi, G. C., Eds.; Delft University Press: Delft, Holland, 1978: pp 64-71.

Photochemical Isomerization of Metal Ethene to Metal Vinyl Hydride Complexes: A Matrix-Isolation and Solution NMR Study

Tanachat W. Bell,[1] David M. Haddleton,[1a] Andrew McCamley,[1b] Martin G. Partridge,[1] Robin N. Perutz,*[,1] and Helge Willner[2]

Contribution from the Department of Chemistry, University of York, York YO1 5DD, U.K., and The Anorganisch-Chemisches Institut der Universität Hannover, Callinstr 9, 3000 Hannover 1, FRG. *Received May 31, 1990*

Abstract: $CpRh(PMe_3)(C_2H_4)$ (**1**), $CpIr(PMe_3)(C_2H_4)$ (**6**), and $CpIr(C_2H_4)_2$ (**8**) ($Cp = \eta^5$-C_5H_5) are isomerized on photolysis in argon matrices at 12-20 K to metal vinyl hydride complexes $CpM(L)(C_2H_3)H$ ($L = PMe_3$, C_2H_4). The products are identified by their characteristic metal hydride and vinyl group vibrations in the IR spectra and by the effect of ^2H-labeling experiments. The same products may be generated by photolysis of a frozen toluene solution at 77 K (**1** and **8**) or a cold toluene solution (**6**) and characterized by ^1H, ^{13}C, and ^{31}P NMR. The vinyl hydride complexes exhibit a wide range of thermal stabilities isomerizing to their precursors at the following temperatures: $CpRh(PMe_3)(C_2H_3)H$ at ~253 K, $CpIr(PMe_3)(C_2H_3)H$ at ~393 K, $CpIr(C_2H_4)(C_2H_3)H$ at ~273 K. Photolysis of **1** in toluene solution at 188 K generates a mixture of $CpRh(PMe_3)(C_2H_3)H$ and isomers of $CpRh(PMe_3)(tolyl)H$; at higher temperatures only insertion into toluene C-H bonds is observed. These and other studies lead to the proposal of an intermediate cage complex, $[CpM(L)\cdots C_2H_4]$, in the isomerization pathway. The reaction mechanism tends toward the intramolecular limit in the order **1** < **8** < **6**. Secondary photolysis of $CpIr(C_2H_4)(C_2H_3)H$ in Ar matrices causes ethene loss and formation of a product identified as the vinylidene complex $CpIr(C{=}CH_2)H_2$. Photolysis of **8** in CO and N_2 matrices leads to substitution products $CpIr(C_2H_4)L$ ($L = CO$, N_2), $CpIr(CO)(C_2H_3)H$, and $CpIr(C_2H_4)(C_2H_3)H$. Photolysis of **1** in CO matrices generates $CpRh(PMe_3)CO$ only; use of N_2 matrices results in formation of $CpRh(PMe_3)N_2$ and $CpRh(PMe_3)(C_2H_3)H$. The photoproducts of **6** in CO matrices include $CpIr(PMe_3)(C_2H_3)H$ and $CpIr(PMe_3)CO$.

Introduction

It was first reported in 1971 that a metal alkene complex could be isomerized on photolysis (eq 1).[3]

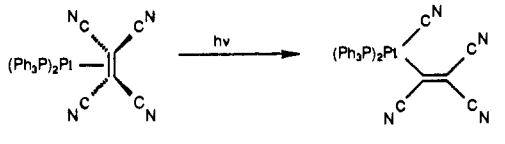

(1)

Evidence that a similar process could occur for an ethene complex came from the measurements of Kafafi et al. on $Fe(C_2H_4)$ isolated in low-temperature matrices.[4] Yet this appeared to be a special case, since $Fe(C_2H_4)$ is hydrogen bonded not π-bound. Nevertheless, this observation was followed in 1986 by Baker and Field's discovery[5] of the photoisomerization of $Fe(dmpe)_2(C_2H_4)$, our own[6] for $CpIr(C_2H_4)_2$ and Wenzel and Bergman's[7] for $CpRe(PMe_3)_2(C_2H_4)$, all conventionally π-bound ethene complexes (dmpe = $Me_2PCH_2CH_2PMe_2$, $Cp = \eta^5$-C_5H_5). The discovery of further examples of metal ethene to metal vinyl hydride isomerization (eq 2a and Scheme I) made it clear that this was far from an isolated phenomenon.[8-10] Although reaction 2a

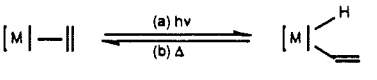

(2)

(1) University of York: (a) Present Address, ICI Chemicals and Polymers Ltd, Runcorn, U.K. (b) Present address, School of Molecular Sciences, University of Sussex, Brighton BN1 9QJ, U.K.
(2) University of Hannover.
(3) Traverso, O.; Carassiti, V.; Graziani, M.; Belluco, U. *J. Organomet. Chem.* **1973**, *57*, C22. Baddley, W. H.; Panattoni, C.; Bandoli, G.; Clemente, D. A.; Belluco, U. *J. Am. Chem. Soc.* **1971**, *93*, 5590.
(4) Kafafi, Z. H.; Hauge, R. H.; Margrave, J. L. *J. Am. Chem. Soc.* **1985**, *107*, 7550.
(5) Baker, M. V.; Field, L. D. *J. Am. Chem. Soc.* **1986**, *108*, 7433, 7436.
(6) Haddleton, D. M.; Perutz, R. N. *J. Chem. Soc., Chem. Commun.* **1986**, 1734.
(7) Wenzel, T. T.; Bergman, R. G. *J. Am. Chem. Soc.* **1986**, *108*, 4856.
(8) Stoutland, P. O.; Bergman, R. G. *J. Am. Chem. Soc.* **1988**, *110*, 5732.
(9) Tanke, R. S.; Crabtree, R. H. *Inorg. Chem.* **1989**, *28*, 3444.
(10) McCamley, A.; Perutz, R. N.; Stahl, S.; Werner, H. *Angew. Chem., Int. Ed. Engl.* **1989**, *28*, 1690.

0002-7863/90/1512-9212$02.50/0